NASA TECHNICAL MEMORANDUM

NASA TM X-1510

NASA TM X-1510

POTENTIAL USE OF HIGH-FREQUENCY INDUCTION HEATING FOR HIGH-TEMPERATURE LIQUID-METAL HEAT-TRANSFER TESTING

by John V. Miller

Lewis Research Center

Cleveland, Ohio

NATIONAL AERONAUTICS AND SPACE ADMINISTRATION • WASHINGTON, D. C. • FEBRUARY 1968

NASA TM X-1510

POTENTIAL USE OF HIGH-FREQUENCY INDUCTION HEATING FOR HIGH-TEMPERATURE LIQUID-METAL HEAT-TRANSFER TESTING

By John V. Miller

Lewis Research Center
Cleveland, Ohio

NATIONAL AERONAUTICS AND SPACE ADMINISTRATION

For sale by the Clearinghouse for Federal Scientific and Technical Information
Springfield, Virginia 22151 – CFSTI price $3.00

POTENTIAL USE OF HIGH-FREQUENCY INDUCTION HEATING FOR HIGH-TEMPERATURE LIQUID-METAL HEAT-TRANSFER TESTING

by John V. Miller

Lewis Research Center

SUMMARY

Experimental determination of the local heat-transfer coefficients of liquid metals at temperatures in excess of 1000° K is very difficult. Not only must the heaters used in the test operate at a temperature where structural strength is low, but also, because of the corrosiveness of liquid metals at these temperatures, the test section must be made of a refractory metal and, therefore, be operated in a controlled environment to prevent oxidation.

To investigate potential methods of obtaining high-temperature liquid-metal heat-transfer data, several possible heating devices have been examined and a cursory summary of the problems of each are discussed. One method which appears promising is the use of high-frequency induction heating. The advantage of this type of heater is that the heating coil is physically separated from the test section and can be maintained at a much lower temperature than the test section. This allows the coil to be constructed of relatively low-temperature materials.

An analysis of a thick-walled cylinder, internally cooled with flowing liquid metal was performed to evaluate the characteristics of an inductively heated test section. It was assumed that a suitable heating coil could be constructed for this application. The results of this study indicate that, if the ratio of cylinder radius to current depth is greater than 6, internal heat generation in the center of the cylinder is negligible. With a tungsten cylinder, for example, commercially available high-frequency equipment can be used to obtain the necessary cylinder-radius to current-depth ratio without exceeding allowable thermal stress levels which have been established for tungsten.

Neglecting the temperature variation of electrical resistivity in the analysis does not appreciably influence the calculated temperature distribution of a tungsten cylinder since nearly all the induced power is in a region where the temperature and resistivity variations are small. Based on an error analysis of an inductively heated test section, experimental determination of liquid-metal heat-transfer coefficients at high heat-flux levels can be made to an accuracy of ±10 percent for reasonable tolerances on thermocouple placement and temperature measurements. An additional error is introduced if the thermal conductivity of the material used in the test section is not well defined.

INTRODUCTION

Liquid metals are excellent heat-transfer fluids because of their relatively high thermal conductivity, high volumetric heat capacity and low vapor pressure at elevated temperatures. These characteristics make liquid metals ideal candidates for many high-temperature, high heat-flux applications. In particular, the use of liquid metals as coolants for nuclear reactors is being considered extensively for systems requiring coolant temperatures of 1000° to 2000° K. In this temperature range, lithium, sodium, potassium, rubidium, cesium, and a mixture of sodium and potassium (NaK) appear to have the necessary qualifications for nuclear reactor coolants (refs. 1 to 3).

In liquid-metal cooled systems, a large portion of the heat transferred is a result of the high molecular conductivity of the coolant. Therefore, heat-transfer correlations for ordinary fluids do not apply since with most other fluids the molecular conductivity is negligible compared with the eddy conductivity.

Much work has already been done in the field of liquid-metal heat transfer. However, the majority of the experimental work has been performed at relatively low temperatures ($<1000^{\circ}$ K) and low heat fluxes (<200 W/cm^2). Extrapolation to higher temperatures and higher heat fluxes should be possible except that there is wide scatter in the available data. Figure 1, for example, shows some of the many heat-transfer relations which have evolved from theoretical (refs. 4 to 6) and experimental (refs. 7 and 8) studies of various liquid metals. Although the form of these and many similar liquid-metal heat-transfer equations vary considerably, they all fall roughly into the region between the Martinelli and Kulateladze equations shown on figure 1.

Generally, the maximum variation in the predicted heat-transfer coefficient is about

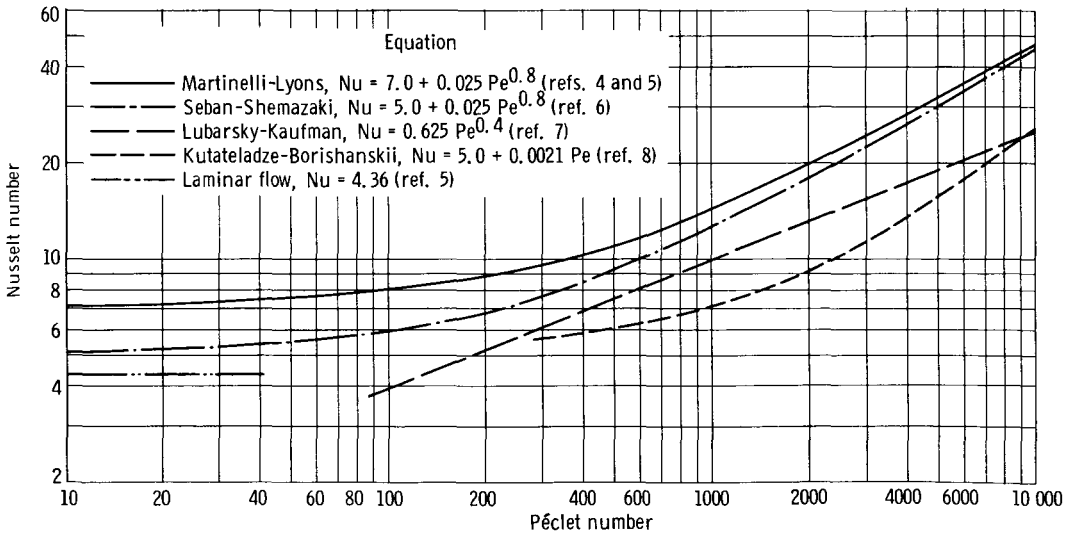

Figure 1. - Comparisons of typical heat-transfer equations for liquid metals.

a factor of 2 or varies by ±35 percent about an average line which could be constructed for the various relations (e.g., at a Péclet number of 1000, the predicted heat-transfer coefficient for lithium flowing in a 5-mm tube at 1000° K is about 12 ± 4 W/cm^2-$^{\circ}$K). For many applications, this ±35 percent accuracy is sufficient. At a heat flux of 100 watts per square centimeter and a nominal heat-transfer coefficient of 5 watts per square centimeter per $^{\circ}$K, for example, the difference between the fluid temperature and predicted surface temperature is $20^{\circ}\pm7^{\circ}$ K. The relatively small error ($\pm7^{\circ}$ K) could be considered negligible for cases in which such temperature differences were not critical. For advanced nuclear reactors, however, heat fluxes in excess of 400 watts per square centimeter and possibly as high as 800 to 1000 watts per square centimeter are desirable to increase the specific power output and/or to minimize the size and weight of a given reactor system, particularly for space-power applications where weight is at a premium. At these high heat fluxes, a ±35 percent error in predicting a nominal heat-transfer coefficient of 5 watts per square centimeter per $^{\circ}$K could result in an error of more than 50° K which, under certain conditions, could result in a reactor fuel element exceeding some limiting heat-transfer or material strength criteria. For example, if a lithium cooled reactor were operating at a coolant temperature of 1750° K and at a pressure of 3 atmospheres (3.03×10^5 N/m^2), a 50° K error in predicting the surface temperature could produce a film boiling burnout condition (ref. 9) since the surface temperature could be higher than the saturation temperature of lithium at that pressure (i.e., $>1790^{\circ}$ K). To prevent such adverse situations, it appears that additional liquid-metal heat-transfer experiments will be required to refine the present data if very high specific power reactors are to be developed.

The reasons for the wide scatter in presently available liquid-metal heat-transfer data are varied.

(1) It is difficult to obtain accurate heat-transfer data at high temperatures and heat fluxes because of instrumentation problems.

(2) For liquid-metal heat-transfer tests, the system must be clean and free from oxides and other contaminants. Much of the scatter in the data has been attributed to the fact that this condition has not always been achieved (ref. 10).

(3) Another important factor, which is of special concern at the high temperatures of interest for nuclear reactors, is that the high corrosivity of liquid-metals dictates the use of refractory metals (i.e., niobium, molybdenum, tantalum, or tungsten) and some of their alloys as the material of construction. Since the refractory metals are susceptible to oxidation, they must be used in a controlled environment (inert gas or vacuum) further increasing an already difficult instrumentation problem.

The instrumentation problem is not merely related to the ability to accurately measure temperatures under high flux and temperature conditions, but it also involves selection of the best locations for measuring temperatures in the test and the accuracy of

thermocouple placement. This factor has several aspects which are peculiar to the various methods used to obtain heat-transfer data in liquid-metal systems. The purpose of this report is to briefly discuss some of these methods and to explore the potential use of high-frequency induction heating for liquid-metal heat-transfer testing.

METHODS OF OBTAINING LIQUID-METAL HEAT-TRANSFER DATA

The task of obtaining reliable experimental heat-transfer data for liquid metals at high temperatures is more difficult as the temperature level increases. At the temperatures of interest for space-power nuclear reactors (1000° to 2000° K), even the selection of the best method of testing is difficult. Because the liquid metals are to be tested at a high temperature (e.g., 2000° K), the test section and heater must be at a significantly higher temperature in order to obtain the required 400- to 1000-watts per square centimeter heat flux.

Although there are several methods of testing which can possibly be applied to liquid-metal heat transfer, the high-temperature problem limits the applicability of many of these methods and reduces the effectiveness of others. Some of these testing methods and their related problems are discussed in the following sections.

Resistance Heating

Probably one of the most widely used methods of obtaining heat-transfer data is the use of direct resistance heating of the test section using direct-current or low-frequency alternating-current voltage. In such a system, the coolant is circulated through a relatively thin-walled tube, a section of which serves as both heater and test section. Thermocouples are attached to the outer surface. The heat-transfer coefficient between tube and coolant is determined from the temperature measurements and a heat balance of the system.

Obviously, since the thermocouples are on the outside of the tube, the temperature of the inside (heat transfer) surface must be estimated. This could lead to a significant error in the predicted heat-transfer rate, particularly for large heat fluxes and temperature gradients. However, for applications in which the fluid being tested is not a good electrical conductor, this method has been used successfully to determine the heat-transfer characteristics of gases (ref. 11) and of liquids such as water (ref. 12). But, when the fluid being studied is a very good electrical conductor, such as is the case of liquid metals, the current being applied is split between the flowing fluid and the test section. A portion of the total heat load is, therefore, generated directly in the coolant.

It would be necessary to correct the temperatures and surface heat flux accordingly to accurately establish the heat-transfer coefficient. Because the determination of the electrical current split between test section and fluid requires knowledge of the electrical resistivity of both materials and because the resistivities are generally temperature dependent, an accurate correction is, in practice, very difficult.

Insulated Resistance Heating

One method of overcoming the current shunting problem would be to separate the liquid-metal coolant from the electrically heated test section by use of an electrical insulator. Several such systems have been designed and tested. One of them uses a 0.3-centimeter-diameter tantalum heater, insulated from a 0.95-centimeter-diameter niobium-zirconium sheath by 0.18 centimeter of swaged alumina (ref. 13). This heater has operated 500 hours at a surface flux of 20 watts per square centimeter with a centerline temperature of approximately 1700° K. Even with this relatively thick insulator some electrical leakage occurred; the effective resistivity of the alumina was reduced to approximately 25 percent of the handbook value.

A second type of resistance heater for liquid-metal systems (ref. 14) consists of a graphite core, approximately 5 centimeters long and 0.3 centimeter in diameter, which is contained in a boron nitride insulator and sheathed in stainless steel. Several of these heaters have operated at fluxes in excess of 470 watts per square centimeter for over 400 hours. The use of stainless steel, of course, limits the allowable coolant temperature to less than 1000° K.

Although further advances in size, heat flux, and allowable operating temperature of these insulated resistance heaters will undoubtedly be achieved, there is one basic factor which limits their application to very high temperatures and heat fluxes. This is the relatively large thermal gradient that will occur across the insulator at high flux levels. For example, at a heat flux of only 500 watts per square centimeter, the temperature drop across a 0.2-centimeter alumina insulator is about 1250° K. If the liquid-metal coolant were operating, for example, at 2000° K, it is obvious that the heater temperature ($>3250^{\circ}$ K) would be well over the melting point of even the refractory metals. Therefore, the use of an insulated electrical heater for high-temperature, high heat-flux applications is limited by the allowable temperature of the heater and, to an extent, by the possible breakdown of the electrical insulating properties of the insulator at high temperatures.

Thick-Wall Resistance Heating

Another way to minimize the current shunting problem without using an insulator is to use a thick-walled rather than a thin-walled tube for the heater and test section. The electrical resistance of any element is proportional to the resistivity and length, and inversely proportional to the cross-sectional area (appendix B). For the case in which the resistivity of the liquid-metal coolant and the thick-walled test section have about the same value, the fraction of heat generated directly in the liquid metal is approximately equal to the ratio of the areas of the coolant passage and the cylinder (i.e., $(q_b/q_t) \cong (a/R)^2$). Figure 2 illustrates how the fraction of heat generated directly in the liquid metal decreases as the thickness of the tube is increased relative to the coolant hole size. When the diameter of the test section is 10 or more times the size of the coolant hole (i.e., $R/a > 10$), over 99 percent of the heat is generated in the tube walls, and the heat generated in the liquid-metal coolant could be considered negligible.

In this illustration (fig. 2), it was assumed that the resistivity of the tube was the same as that of the liquid metal. In practice, such a condition would probably not occur,

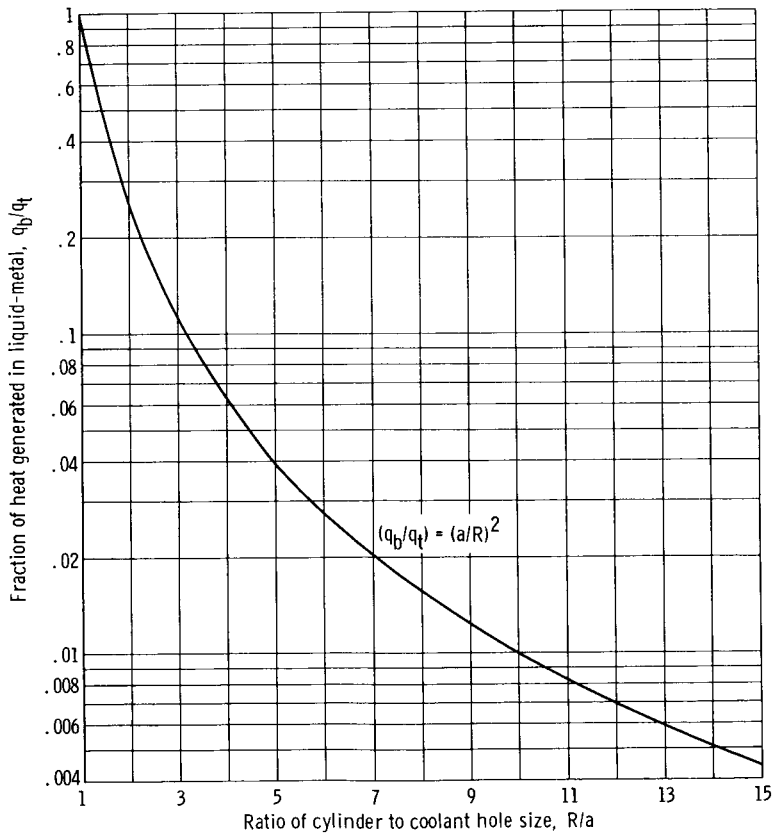

Figure 2. - Effect of cylinder-to-coolant-hole size on heat generated in coolant of resistively heated, liquid-metal-cooled test section assuming that electrical resistivity of liquid metal and the test section are approximately equal.

since, even within the thick-walled cylinder, the resistivity would vary with temperature. This illustration, however, does point out that, by increasing the wall thickness sufficiently, the shunting problem can be neglected.

Because of the thick-walled tube used in this method, it would be impractical to attach thermocouples to the outer surface and make accurate corrections for the temperature on the inside surface. This is apparent from figure 3 where the temperature distribution in a resistively heated cylinder shows a significant difference in the surface temperature for typical conditions which might be encountered in a test. A difference of nearly 70° K exists at the outer surface of the cylinder between the case where all heat generated in the test section is transferred to the fluid ($\epsilon = 1.0$) and the case where 50 percent of the heat is lost by conduction, convection, and radiation from the outer surface.

A more logical method of instrumenting the thick-walled tube would be to drill a hole radially from the outer surface to as near the inner surface as possible. The thermocouple could be then positioned near the inner wall in a location where the thermal efficiency ϵ of the test section does not affect the temperature profile. A heat balance in the liquid-metal coolant could establish both the fluid temperature and heat flux at the same axial location as the thermocouple. This information would suffice to establish the local heat-transfer coefficient. A correction would, of course, be necessary to account for the difference between the actual inside surface temperature and the temperature at

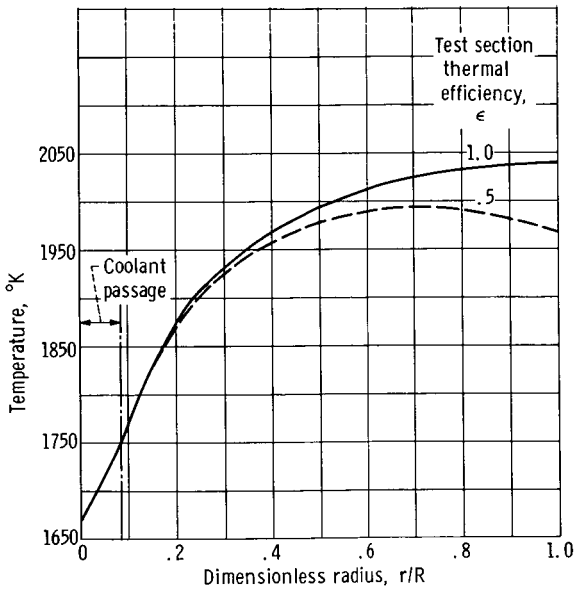

Figure 3. - Typical temperature distributions in resistively heated thick-walled cylinder cooled by liquid metal. Ratio of cylinder to coolant-hole size, 12; radius of coolant channel, 0.32 centimeter; bulk fluid temperature, 1670° K; heat-transfer coefficient, 6 watts per square centimeter per °K; heat flux, 475 watts per square centimeter.

the thermocouple location. A discussion of the accuracy with which the heat-transfer coefficient can be measured is given in the section ERROR ANALYSIS.

DOUBLE TUBE HEAT EXCHANGER

Average heat-transfer rates can be obtained using a double-tube heat exchanger. In this method an inner tube serves as a carrier for one fluid, while a second fluid passes through the annulus formed by the two tubes. Heat transfer from the second fluid to the inner tube can be by single-phase convection or by condensation of a vapor on the outer wall of the inner tube. The secondary fluid may or may not be the same as the primary fluid in the first case; it may actually be the identical fluid which is pumped in series through both the outer and inner tube. In the case where the fluids are different, the secondary fluid may even be a gas, although it would require a substantial flow of gas to provide the necessary heat-transfer coefficient and heat capacity to supply the required heat load to the liquid metal.

The chief problem with this system is that it is impractical to attach thermocouples on the inner tube. Temperatures measured on the outer surface of the outer tube would need considerable correction to obtain a local heat-transfer coefficient for the inner tube.

Thermal-Radiation Heaters

The thermal-radiation heater is one in which the heat transfer to the test section is by thermal radiation from a much hotter heat source. One such heater has been designed (ref. 13) to produce about 20 watts per square centimeter at 1000° K.

The main disadvantage of this type of heater to high-temperature, high heat-flux applications is the very high operating temperature of the heater. For example, at a coolant temperature of about 1500° K, the required heater temperature for a thermal-radiation device would be over 3500° K to deliver 1000 watts per square centimeter using the ideal black-body equation (ref. 15):

$$\varphi = F\sigma\left(T_h^4 - T_o^4\right) \tag{1}$$

(Symbols are defined in appendix A.)

Electron-Bombardment Heating

An electron-bombardment heater consisting of an evacuated tube in which a stream of electrons were directed against the inner wall has been used (ref. 13) with liquid-metal systems. This heater had already operated at 110 watts per square centimeter but only has an expected capability of 300 watts per square centimeter.

One difficulty with electron-bombardment heating is the complexity necessary to ensure a uniform stream of electrons over the entire surface of the test section. For example, to obtain uniform heating on the outside of a round tube it would be necessary to use multiple electron beams to effectively cover the entire surface. Further work on electron-bombardment heaters may eliminate this restriction and improve the performance of this type of heater.

High-Frequency Induction Heating

Another potential method of performing high-temperature heat-transfer tests on liquid metals is the use of high-frequency (>1000 Hz) induction heating. Induction heating is widely used industrially on many configurations for such applications as brazing, annealing, tempering, and many other processes in which localized high-temperature heating effects are required. The rapidly alternating current of such a system results in the so called skin-effect which produces a highly concentrated heating source near the surface of the metal piece. The power input could either be directly coupled across the test section, as is presently done with direct-current or low-frequency alternating current systems, or the more conventional method of inducing a current in the test section by passing a current through a surrounding coil could be used. Because most of the power is generated near the surface, the heat transfer near the center of the test section is essentially a conduction process.

Kalachev, et al. (ref. 16), have investigated the use of induction heating for flowing liquid metals which are to be used as heat-transfer fluids. They have concluded that, for high-temperature application, such a heater has the advantages of smoothly adjustable output, stable heat generation, and a power output which is independent of the temperature of the heated fluid. They have estimated the heat flux capability for this application at about 1000 watts per square centimeter and have recommended induction heating for use in all liquid-metal systems.

However, Kalachev, et al., were mainly interested in using the induction heater as a means of heating the liquid metal. To extend this work to the experimental determination of the local heat-transfer coefficients of liquid metals, it is first necessary to determine the basic thermal and electrical characteristics of an inductively heated test section used

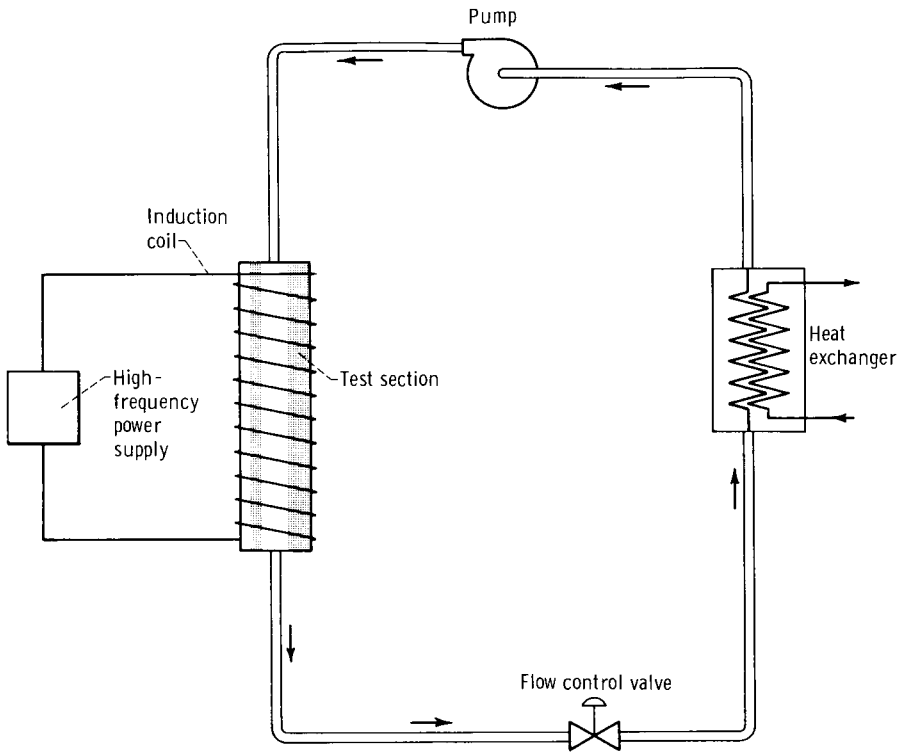

Figure 4. - Diagram of liquid-metal heat-transfer loop using high-frequency induction heating.

for such an application. The resulting temperature distribution and related information obtained from an analysis of an inductively heated test section can be used to define the optimum location for placement of thermocouples to enhance the reliability of the experiment and to reduce the error in determining the heat-transfer coefficient.

Figure 4 schematically illustrates the major components required for an inductively heated system. The coolant loop consists of pump, flow control valve, and a heat exchanger. By regulating the flow rate in the primary coolant loop and in the secondary side of the heat exchanger, the liquid metal could be maintained at some predetermined temperature and flow level for each test.

The instrumented test section is a thick-walled cylinder (fig. 5) surrounded by the high-frequency induction coil. To avoid disturbing the induced electrical field, the thermocouples would probably have to be inserted axially and located near the center of the cylinders in the region where the induced current flow is negligible. This could possibly result in some error due to inaccuracies in locating the thermocouple (see ERROR ANALYSIS).

The advantage of this type of heater is that the induction coil may be physically separated from the test section by insulation or some form of radiation shield to reduce heat losses from the hot test section and to allow the coil to operate at a much lower temperature than the test section. Induction coils are generally constructed of hollow copper tubing, which is water cooled to limit the operating temperature of the copper.

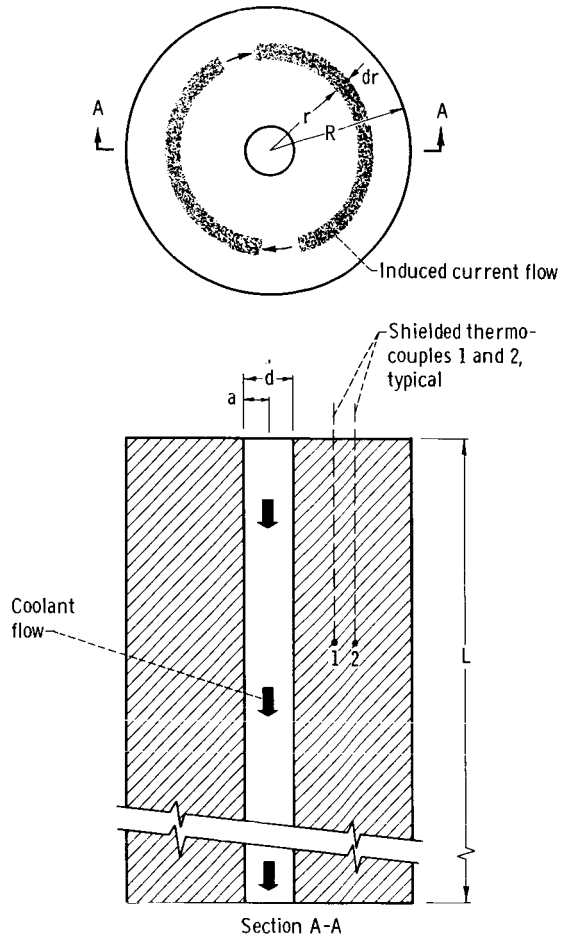

Figure 5. - Test section.

However, because of the temperature difference between test section and the surrounding coil, a portion of the heat generated in the test section is lost from the outer surface of the cylinder. The ratio of the heat actually transferred to the liquid metal to that generated in the test section will be termed the thermal efficiency ϵ of the test section. In addition to the heat loss directly from the test section, other losses occur in the system. One source of such losses is the coil itself. Although induction heating is used quite extensively in many industrial applications, in many cases the actual construction of the coil is an art rather than a true science. To obtain uniform heating and to prevent excessive end losses, the coil must be delicately tuned for each application. However, for a cylindrical test section the construction of a suitable coil does not appear to be a major problem, although the operating frequency must be properly selected to avoid a mismatch between the impedance of the power supply and the test section.

Kalachev, et al. (ref. 16), have measured the overall efficiencies of inductively heated liquid-metal systems at 55 to 75 percent. With such efficiencies, the power requirement for the high-frequency generator would be nearly twice that actually needed

for the test. For example, to transfer 1000 watts per square centimeter to a 25-centimeter-long test section with a 0.5-centimeter coolant-hole diameter, only 39 kilowatts of power would actually be transferred to the liquid metal, but the required power output of the high-frequency generator would be about 70 kilowatts (i.e., using Kalachev's 55 percent overall efficiency). However, this is well within the power levels of commercially available equipment as shown on table I.

TABLE I. - COMMERCIALLY AVAILABLE HIGH-FREQUENCY POWER SUPPLIES

Power supply	Frequency range, kHz (a)	Power output range, kW (a)	Reference
Electronic tube generators	180 to 450	1 to 100	17
Electronic tube generators	2500 to 25 000	2.5 to 50	17
Motor-generators	1 to 10	7.5 to 500	18

[a]Not all combinations of frequency and power are available in the ranges shown.

Therefore, from the standpoint of being able to obtain the necessary power for a liquid-metal heat-transfer test, it appears that presently available commercial equipment could be utilized. It remains necessary to show how well the heat-transfer coefficient of liquid metals can be determined from an inductively heated test section.

ANALYSIS OF INDUCTIVELY HEATED TEST SECTION

Induced Current

The fundamental equation for the distribution of the magnetic-field intensity H in an inductively heated cylinder is (ref. 19)

$$\frac{d^2H}{dr^2} + \frac{1}{r}\frac{dH}{dr} - k^2jH = 0 \tag{2}$$

where k is defined by the relation

$$k^2 = \frac{2\pi f\mu}{\rho_{(T)}} \tag{3}$$

The induced current is related to the magnetic-field intensity by

$$I_{(r)} = \frac{1}{4\pi} \frac{dH}{dr} \tag{4}$$

Since nearly all nonferrous metals have about the same permeability (ref. 20) ($\mu_n = 4\pi \times 10^{-9}$ Wb/A-cm) a thick-walled refractory metal cylinder with a liquid-metal coolant will behave essentially the same as a solid cylinder with respect to the induced current distribution. This is particularly true when nearly all the induced current is near the outer surface of the cylinder, in which case the presence or absence of the coolant in the center of the cylinder is unimportant to the current distribution.

The solution to equations (2) and (4) is complicated by the variation of the electrical resistivity ρ of most metals with temperature. Table II shows the resistivity of some

TABLE II. - RESISTIVITY OF SOME TYPICAL REFRACTORY METALS[a]

Temperature, ^{o}K	Tantalum	Molybdenum	Tungsten
	Resistivity, microhm-cm		
293	-----	5.7	5.51
300	13.85	----	-----
1000	44.1	----	25.3
1023	-----	21.0	-----
1500	-----	----	41.4
2000	-----	----	59.4
3000	-----	----	98.9
3510	-----	----	118.0

[a]Data from ref. 21.

typical refractory metals (data from ref. 21). In the temperature range from 1500^{o} to 3000^{o} K, for example, the resistivity of tungsten can be represented by an equation of the form

$$\rho_{(T)} = \left[2.333 \left(\frac{T}{1000} \right)^2 + 27.83 \left(\frac{T}{1000} \right) - 5.587 \right] \cdot 10^{-6} \text{ ohm-cm} \tag{5}$$

Obviously, substitution of this expression into equation (2) would result in a very complex differential equation. And, since the functional form of the temperature dependency of resistivity is different for each metal, a completely general solution to the inductively heated cylinder would not be possible. To obtain the current distribution in an inductively heated cylinder, therefore, the assumption is made that the resistivity of the cylinder is

independent of temperature. The validity of this assumption can be determined after the complete solution for the inductively heated cylinder, including the resulting temperature profile, has been obtained.

Reference 19 shows that, under the assumption of uniform resistivity, the ratio of the induced current at any radial location r to that induced at the surface of the cylinder is given by

$$\frac{I_{(r)}}{I_o} = \frac{\text{ber}'(kr) + j\,\text{bei}'(kr)}{\text{ber}'(kR) + j\,\text{bei}'(kR)} \tag{6a}$$

where ber and bei are defined, respectively, as the real and imaginary parts of the Bessel function of the first kind of zero order; that is,

$$J_o\left(jkr\sqrt{j}\right) = \text{ber}(kr) + j\,\text{bei}(kr) \tag{7}$$

Values of ber and bei and the derivatives ber' and bei' are tabulated in various forms in references 19, 22, and 23. The induced current distribution may be numerically evaluated using these tables and considering the absolute value of equation (6a); that is,

$$\left|\frac{I_{(r)}}{I_o}\right| = \left[\frac{\text{ber}'^2(kr) + \text{bei}'^2(kr)}{\text{ber}'^2(kR) + \text{bei}'^2(kR)}\right]^{1/2} \tag{6b}$$

Heat Conduction

If the length-to-diameter ratio of the cylinder is large ($L >> d$), the temperature gradient in the axial direction will be small compared with the radial gradient. Under these conditions, axial heat conduction away from the ends of the cylinder can be neglected, and the radial, steady-state heat conduction in the cylinder with internal heat generation (ref. 24) is given by

$$\frac{d^2T}{dr^2} + \frac{1}{r}\frac{dT}{dr} = -\frac{Q_{(r,\,T)}}{K_{(T)}} \tag{8}$$

As in the case of the induced current, the temperature dependency of the properties of the material complicate the solution of the differential equation. Therefore, the as-

sumption is made that the resistivity and thermal conductivity are independent of temperature. The validity of this assumption will also be discussed after the temperature profile has been determined.

Appendix B shows that, for a uniform resistivity, the local volumetric heat-generation rate is related to the induced current by

$$\frac{Q_{(r)}}{Q_o} = \left[\frac{I_{(r)}}{I_o}\right]^2$$

so that

$$Q_{(r)} = Q_o\left[\frac{ber'^2(kr) + bei'^2(kr)}{ber'^2(kR) + bei'^2(kR)}\right] \tag{9}$$

It is obvious that the direct use of equation (9) in the heat conduction equation (eq. (8)) would also result in a rather complex differential equation.

Approximate Solution

Reference 19 notes that for large values of the quantity kR, an approximate form of equation (6a) is given by the exponential expression

$$\frac{I_{(r)}}{I_o} = e^{-k(R-r)/\sqrt{2}} \tag{10a}$$

When the value of R - r is equal to $\sqrt{2}/k$ in this expression (eq. (10a)), the local value of the induced current is reduced by a factor of e or to 36.8 percent the value at the outer surface of the cylinder; that is, when $(R - r) = \sqrt{2}/k$,

$$\frac{I_{(r)}}{I_o} = \frac{1}{e} = 0.368$$

For this reason, the value of $\left(\sqrt{2}/k\right)$ has been termed (ref. 19) the equivalent current depth δ of an inductively heated cylinder and is defined as the depth, relative to the outer surface of the cylinder, at which the induced current is reduced by a factor e.

TABLE III. - VARIATION IN INDUCED CURRENT AND VOLUMETRIC HEAT GENERATION RATE OF INDUCTIVELY HEATED CYLINDER WITH INCREMENTAL VALUES OF EQUIVALENT CURRENT DEPTH

Incremental value of equivalent current depth[a]	Relative value of induced current[b]	Relative value of heat generation rate[b]
1	0.3679	1.354×10^{-1}
2	.1353	1.83×10^{-2}
3	.0498	2.5×10^{-3}
4	.0183	3.0×10^{-4}
5	.0067	$<10^{-4}$
6	.0025	$<10^{-5}$
7	.0009	$<10^{-6}$
8	.0003	$<10^{-7}$

[a]Measured from outer surface of cylinder.

[b]Relative to the value at outer surface of cylinder.

(For each successive incremental δ distance, the current is reduced by a factor of e^n as shown on table III.)

Equation (10a) can be rewritten in terms of this defined variable δ.

$$\frac{I_{(r)}}{I_o} = e^{-(R-r)/\delta} \tag{10b}$$

where

$$\delta = \frac{\sqrt{2}}{k} = \left(\frac{\rho}{\pi\mu f}\right)^{1/2} \tag{11a}$$

which, for the case of nonferrous materials ($\mu = 4\pi\times10^{-9}$ Wb/A-cm), can be expressed as

$$\delta = 5033.7\left(\frac{\rho}{f}\right)^{1/2} \tag{11b}$$

A plot of the variation in induced current with cylinder radius is shown on figure 6 for several values of the dimensionless ratio R/δ. It can be seen that, for the larger values of R/δ, the induced current is reduced to a negligible value in a relatively short distance.

Because the volumetric heat-generation rate is related to the square of the induced current (eq. (9)), the falloff in heat generation is even more rapid (table III). Figure 7

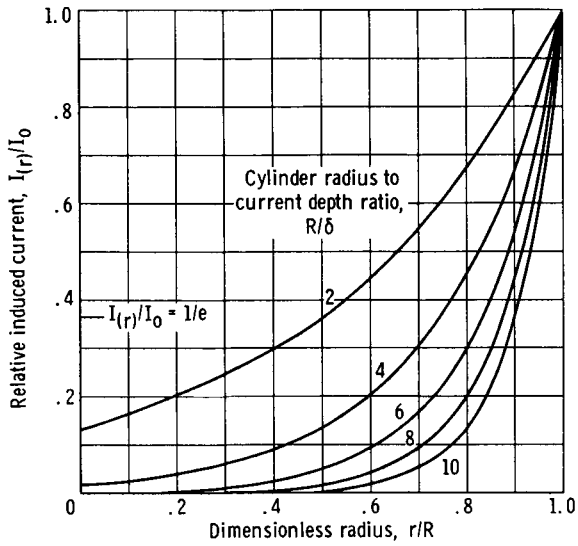

Figure 6. - Variation in induced current with radius and cylinder radius to current depth ratio using approximate solution (eq. (10b)).

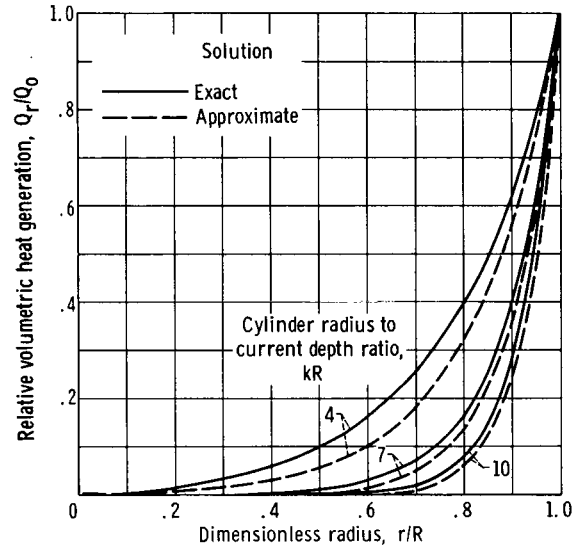

Figure 7. - Comparison between exact and approximate solution of volumetric heat-generation distribution in cylindrical body located in high-frequency induction coil.

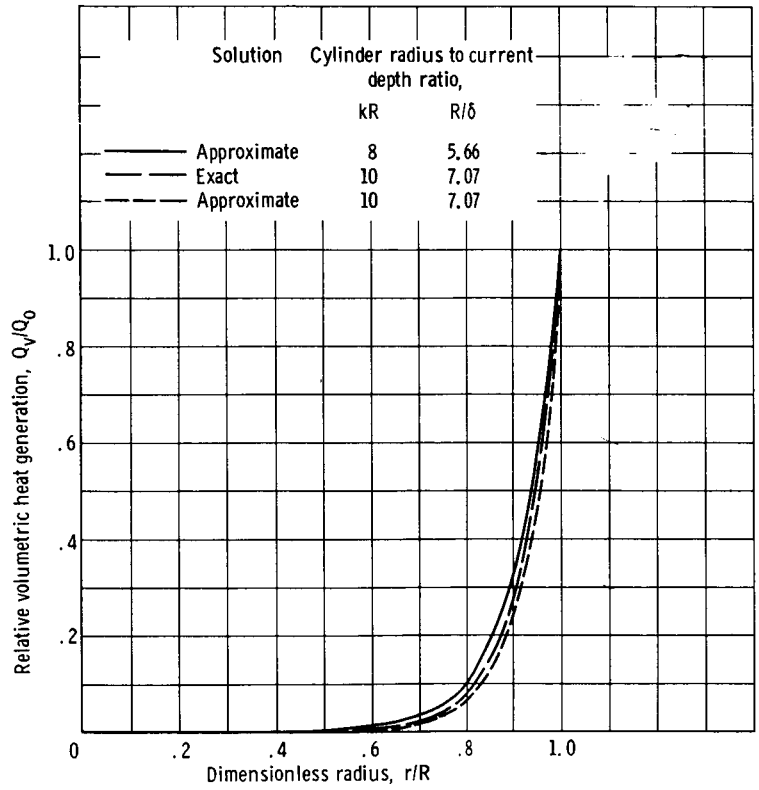

Figure 8. - Relation between exact and approximate volumetric heat-generation distribution for cylindrical distribution for cylindrical body located in high-frequency induction coil.

illustrates this point and also compares the volumetric heat-generation distribution obtained using the exact solution (eq. (9)) and that obtained using the approximate form of the current distribution (eq. (12)):

$$\frac{Q_{(r)}}{Q_o} = e^{-2(R-r)/\delta} \tag{12}$$

For the larger values of R/δ, the absolute difference between the exact and approximate solutions is small. Equally important, the exact solution for a given value of R/δ lies between the approximate solution for that and another value of R/δ. This can be seen more readily in figure 8, where the exact solution for $kR = 10$ lies between the approximate solutions of $kR = 8$ and $kR = 10$. This is an important factor since, as will be shown, the resulting temperature distributions for either value ($kR = 8$ or $kR = 10$) is essentially identical in certain regions of the cylinder. Therefore, since these two approximate solutions bracket the exact solution for $kR = 10$, the temperature distribution for the exact solution would also be identical in these regions.

TEMPERATURE DISTRIBUTION

Using the approximate solution for the volumetric heat generation (eq. (12)), the solution for the radial temperature distribution in an inductively heated cylinder is derived in appendix B. The result, in terms of the dimensionless temperature difference

$$\Delta T_{(r)} = \frac{K\left[T_{(r)} - T_a\right]}{a\varphi_a} \tag{13}$$

is given by

$$\Delta T_{(r)} = \ln\left(\frac{r}{a}\right) + \frac{1}{\epsilon}\left\{\frac{e^x\left[1 + x\ln\left(\frac{r}{a}\right)\right] - e^{xr/a} + \sum_{n=1}^{\infty}\frac{\left[\left(X\frac{r}{a}\right)^n - X^n\right]}{n\cdot n!} - \ln\left(\frac{r}{a}\right)\sum_{n=1}^{\infty}\frac{X^n}{n!}}{e^y(y-1)+1}\right\} \tag{14}$$

where

$$x = 2\frac{a}{\delta}$$

$$y = 2\frac{R}{\delta}$$

and ϵ is the thermal efficiency of test section (i.e., the ratio of heat actually entering the coolant to total heat generated in test section).

Figure 9 shows the radial temperature distribution which results from applying the dimensionless expression (eq. (14)) to a set of conditions which might be typical of an inductively heated test section. Figure 9(a) shows the variation in temperature for several values of the dimensionless ratio R/δ. Also shown in figure 9(a) is the temperature distribution which would result if the heat transfer from the outer surface of the cylinder to the coolant were only by conduction (i.e., no internal heat generation). Note that, for larger values of R/δ, the temperature distribution in the inductively heated cylinder ap-

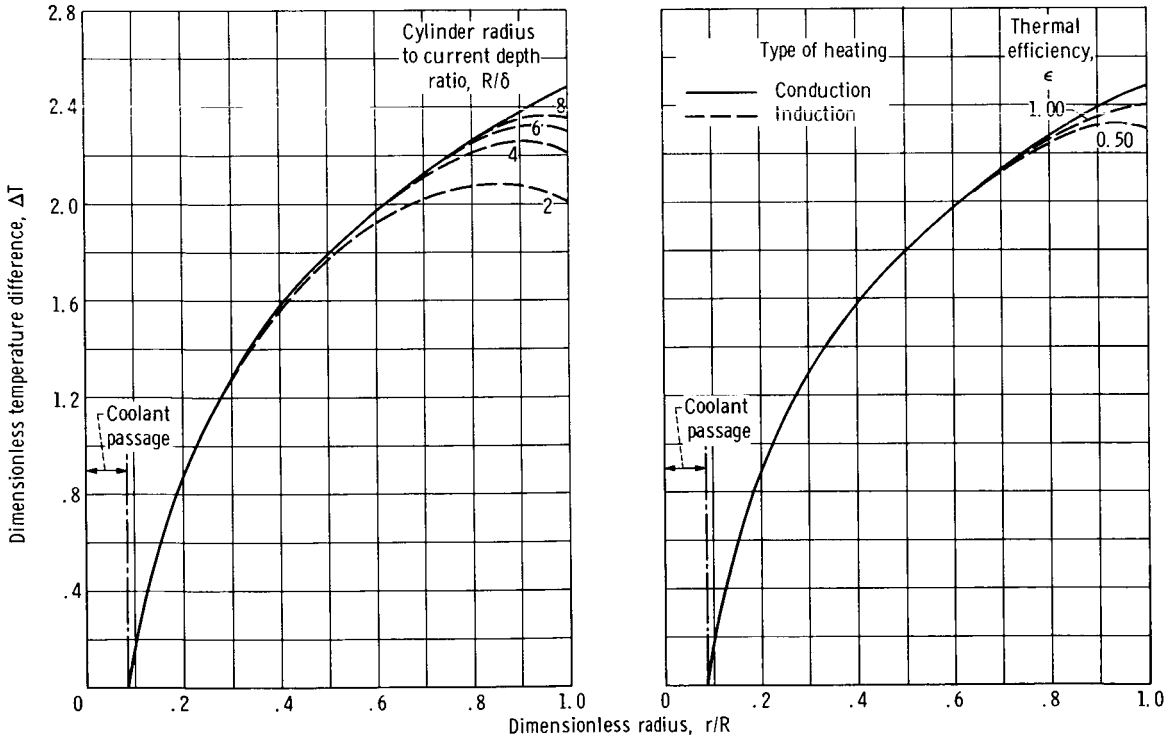

(a) For several values of ratio of cylinder radius to current depth. Thermal efficiency, 0.50.

(b) For test section thermal efficiencies of 0.50 and 1.00. Ratio of cylinder radius to current depth, 6.

Figure 9. - Radial temperature distribution in inductively heated cylinder. Ratio of cylinder radius to coolant hole size, 12.

proaches that of the conduction distribution. Conversely, as the value of R/δ decreases, the temperature distribution becomes more like that of the thick-walled resistively heated cylinder (fig. 3).

These temperature profiles (fig. 9(a)) were determined using a test section efficiency of 50 percent; that is, half of the heat generated in the test section actually enters the coolant and half is lost from the outer surface of the cylinder. Although the power requirement of the test section is inversely proportional to this efficiency, figure 9(b) shows that, for large values of R/δ, the effect of test section efficiency on the temperature distribution of an inductively heated cylinder is small. In fact, in the region $r/R < 0.6$, there is essentially no difference among the temperature distributions of (1) an inductively heated cylinder with a test section thermal efficiency of 0.5, (2) an inductively heated cylinder with a test section thermal efficiency of 1.0, or (3) a cylinder in which heat transfer is by conduction only. The reason for this similarity is shown on figure 10 where lines of constant power-input for an inductively heated cylinder are shown as a function of cylinder radius and the ratio R/δ. For values of $R/\delta > 6$, over 99 percent of the total heat is generated in the region $0.6 < r/R < 1.0$. Therefore, for a given heat load to the coolant, the temperature distribution in the region $r/R < 0.6$ is essentially that of a conduction process and is independent of conditions near the outer surface of the cylinder. This behavior is an important factor in the application of induction heating to heat-transfer testing.

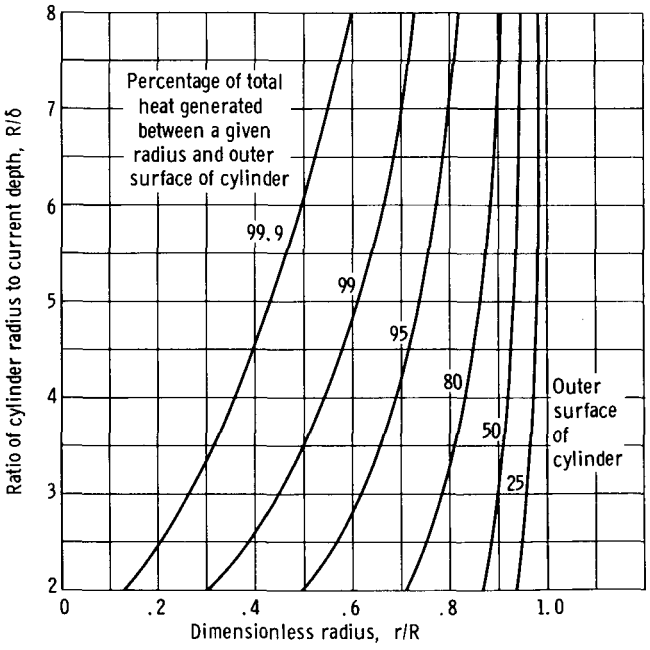

Figure 10. - Lines of constant power output for inductively heated cylinder. Percentage of heat generated between a given radius and outer surface of cylinder.

APPLICATION TO HEAT TRANSFER TESTING

In applying induction heating to tests in which local heat-transfer coefficients are to be determined, it is necessary to establish

(1) The heat flux

(2) The surface temperature of the coolant passage

(3) The coolant temperature

Ideally, for purposes of correlating experimental data, it would be desirable to assume that the heat generation within the cylinder is negligible and that the heat transfer from the outer surface of the cylinder to the coolant channel was by conduction only. As already demonstrated (figs. 7 to 10), this is a fair assumption provided that the ratio of cylinder radius to current depth R/δ is properly chosen. For values of R/δ greater than 6, the temperature distribution in the region $a/R < r/R < 0.6$ is essentially the same as that which would result from heat conduction through a thick-walled cylinder with no internal heat generation.

The heat flux can be determined by measuring the temperature difference between two thermocouples located in this region ($a/R < r/R < 0.6$) and applying the heat conduction equation (ref. 24) for an internally cooled cylinder,

$$\varphi_a = \frac{K(T_2 - T_1)}{a \ln\left(\frac{r_2}{r_1}\right)} \tag{15}$$

where the subscripts 1 and 2 refer to thermocouple locations (fig. 5).

When equation (15) is rewritten in terms of the coolant-channel surface, the temperature at the inner surface of the thick-walled cylinder can be determined using either of the two thermocouples as a reference

$$T_a = T_2 - \frac{\varphi_a \, a \ln\left(\frac{r_2}{a}\right)}{K} \tag{16}$$

The coolant temperature at the axial location of interest can be measured directly or, can be established by measuring the inlet- and exit-coolant temperature and assuming a linear temperature rise across the test section. (Note that this method can be used in conjunction with the flow rate to check the heat flux.)

Once these three parameters φ_a, T_a, and T_b have been established, the heat-transfer coefficient can be calculated from the relation

$$h = \frac{\varphi_a}{(T_a - T_b)} \tag{17}$$

The only restriction to using the above method of obtaining heat-transfer data for an inductively heated cylinder is the requirement that the R/δ ratio be sufficiently large to ensure that the heat-generation rate in the region of the thermocouples is negligible. There are two ways in which the ratio R/δ can be altered to obtain the required value ($R/\delta > 6$): either the diameter of the cylinder can be increased, or the equivalent current depth can be decreased. Obviously, the advantage of using a large diameter cylinder for the test section is that it provides additional cross-sectional area to facilitate the placement of thermocouples (fig. 5). However, the larger the diameter of the cylinder, the greater will be the temperature gradient through the test section for a given power input to the coolant. For example, for a 5-, 7.5-, and 10-centimeter tungsten cylinder, the temperature gradients associated with a 500-watt-per-square-centimeter heat flux at the surface of a 0.75-centimeter cooling hole are 435°, 580°, and 685° K, respectively. Although it is not clear that such gradients could not be tolerated, the thermal stresses imposed, particularly for cyclic operation, could result in test section failure.

Fiero (ref. 25) has established allowable temperature gradients for tungsten based on cyclic strain data. It appears that, for 25 to 50 cycles, temperature gradients of approximately 500° K could be tolerated without test section failure. Therefore, depending on heat flux and coolant-hole diameter, tungsten cylinders of about 6 to 8 centimeters in diameter could be utilized for an inductively heated test section. To maintain a radius-to-current depth ratio R/δ of 6 or more for cylinders of this size, it would be necessary to keep the equivalent current depth below 0.5 to 0.67 centimeter. Figure 11 shows a plot of required frequency necessary to obtain various current depths. Over the temperature range of interest (1000° to 2000° K), the minimum frequency necessary to maintain the required current depth ($\delta < 0.67$ cm) is 1500 hertz. At frequencies above this value, the equivalent current depth is decreased, and the resulting R/δ ratio is further improved (i.e., increased to values greater than 6). Since this frequency range (i.e., >1500 Hz) is available on commercial equipment (table I), inductively heated tungsten cylinders, 6 to 8 centimeters in diameter, appear feasible for a liquid-metal heat-transfer test section. Table IV lists the characteristics of a typical tungsten test section for an arbitrary set of conditions.

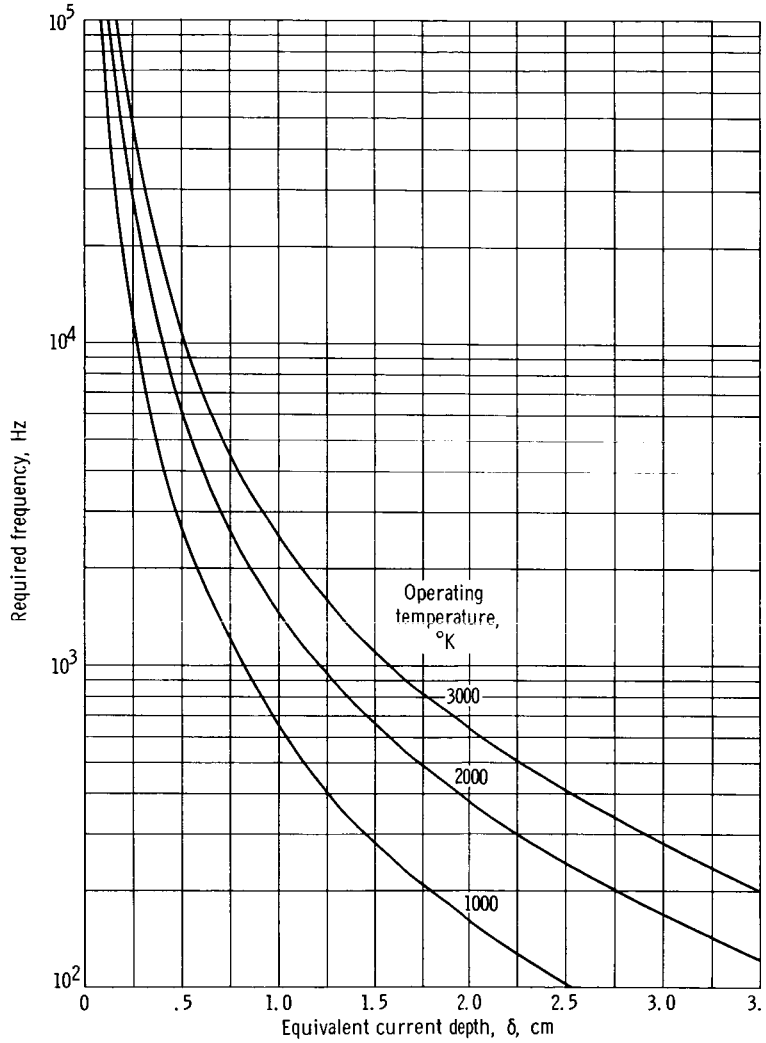

Figure 11. - Required frequency necessary to maintain various current depths in inductively heated tungsten cylinder at several operating temperatures.

TABLE IV. - TYPICAL CHARACTERISTICS[a] OF AN INDUCTIVELY HEATED TUNGSTEN TEST SECTION FOR LIQUID-METAL HEAT-TRANSFER TESTING

(a) General characteristics

Coolant hole diameter, cm	0.64
Test section length, cm	25
Heat-transfer area, cm^2	50
Outside diameter of test section, cm	7.68
Test section-to-coolant hole ratio	12
Minimum cylinder radius-to-current depth ratio	6
Maximum allowable current depth, cm	0.64
Required operating frequency, Hz	[b]3500
Average liquid-metal temperature, ^oK	1670
Heat flux to coolant, W/cm^2	475
Heat-transfer coefficient, $W/(cm^2)(^oK)$	6
Surface temperature of coolant channel, ^oK	1750
Effective thermal conductivity of test section, $W/(cm)(^oK)$	[b]1.03

(b) Power requirements as function of thermal efficiency

Power requirements	Thermal efficiency of test section, percent	
	100	50
Maximum test section temperature, ^oK	2100	2090
Power required by test section, kW	23.75	47.50
Minimum power supply requirement,[c] kW	31	62

[a]For arbitrary set of conditions.

[b]Assuming an average test section temperature of 2000^o K.

[c]Assuming a 30-percent loss in power supply and heating coil.

ERROR ANALYSIS

The local heat-transfer coefficient of an inductively heated, liquid-metal cooled cylinder can be determined using the methods outlined in the previous section. However, the accuracy with which the heat-transfer coefficient can be established depends on several factors.

Temperature Variation of Properties

The first item which could influence the accuracy of determining the heat-transfer coefficient, and the most important to this analysis, is the extent to which the assumption

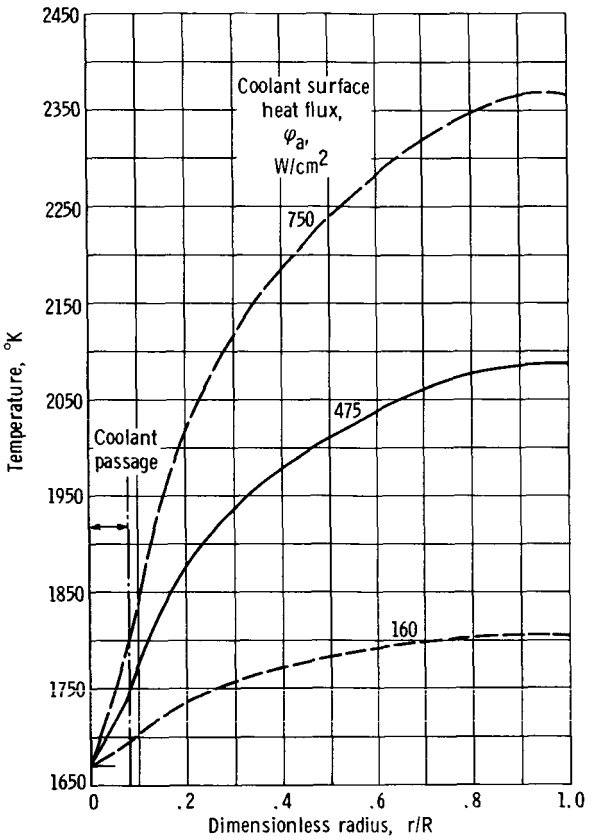

Figure 12. - Typical temperature distributions in inductively heated tungsten, thick-walled cylinder convectively cooled by liquid metal. Ratio of cylinder radius to current depth, 6; ratio of cylinder radius to coolant-hole size, 12; radius of coolant channel, 0.32 centimeters; thermal efficiency, 0.50; bulk fluid temperature, 1670° K; heat-transfer coefficient, 6 watts per square centimeter per °K.

of constant resistivity and constant thermal conductivity can be applied.

Figure 12 shows typical temperature distributions in an inductively heated tungsten cylinder for conditions which might be encountered in a liquid-metal heat-transfer test. These temperature distributions were determined using the equation which was derived with the assumption of constant properties (eq. (14)). The variation in electrical resistivity of tungsten with temperature has already been given (eq. (5)). A similar equation (ref. 26), expressing the thermal conductivity of tungsten in the temperature range of interest, is given by

$$K_{(T)} = 133.8 - 15.6\frac{T}{1000} \quad W/(m)(^{O}K) \tag{18}$$

Although the slope of the temperature distribution in the inductively heated cylinder

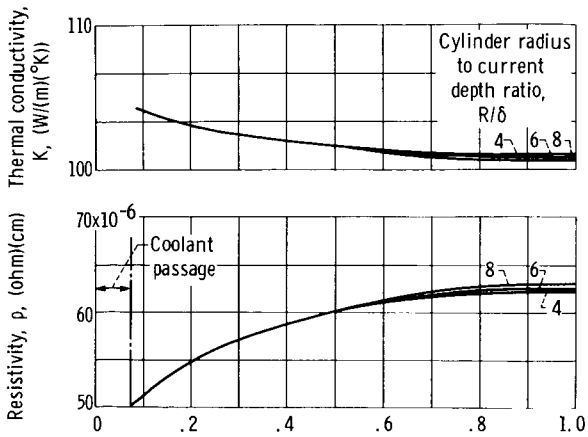

(a) For several ratios of cylinder radius to current depth. Ratio of cylinder radius to coolant-hole size, 12; heat flux, 475 watts per square centimeter; thermal efficiency, 0.50.

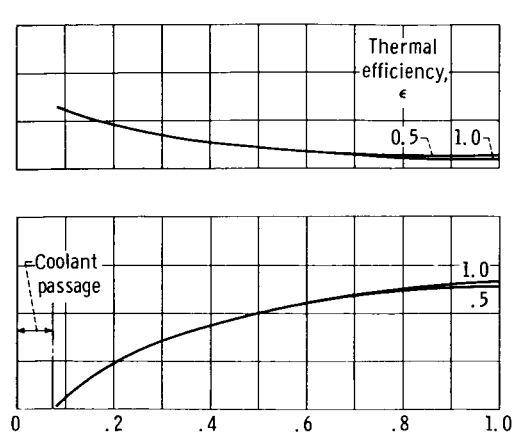

(b) For test section thermal efficiencies of 0.50 and 1.0. Ratio of cylinder radius to current depth, 6; ratio of cylinder radius to coolant-hole size, 12; heat flux, 475 watts per square centimeter.

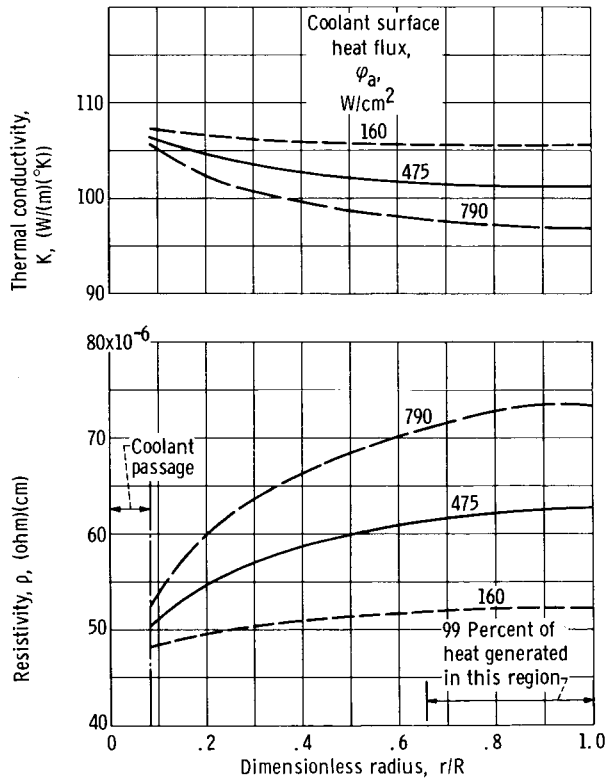

(c) For several heat-flux levels. Ratio of cylinder radius to current depth, 6; ratio of cylinder radius to coolant-hole size, 12; thermal efficiency, 0.50.

Figure 13. - Variation in resistivity and thermal conductivity with test section radius. Radius of coolant channel, 0.32 centimeter; bulk fluid temperature, 1670° K; heat-transfer coefficient, 6 watt per square centimeter per °K.

appears to be quite steep, particularly for high values of heat flux (fig. 12), the resulting variation in the properties is not. Figure 13 shows the variation is thermal conductivity and electrical resistivity across the cylinder for various values of R/δ, thermal efficiency ϵ and heat flux. The extreme variation in thermal conductivity for the worst case shown (i.e., for the highest heat flux) is less than 10 percent; for lower values of heat flux the variation is even less.

In the case of the electrical resistivity, the gross variation across the cylinder is on the order of 40 percent for the high heat flux case (fig. 13(c)). However, in the region where most of the heat is generated and where the variation in resistivity is important, the variation about a mean value of resistivity is only ±2 percent for the 790-watt-per-square-centimeter heat-flux case and ±1 percent for the 475-watt-per-square-centimeter case under the conditions shown. (Note that even if the heat-transfer coefficient were changed by a factor of 2 from the 6 $W/(cm^2)(^oK)$ used in this example, the absolute temperature level would only change by a small amount because the temperature difference between surface and coolant is small compared with the temperature drop through the tungsten. At 475 W/cm^2, for example, the temperature level would only change by 40^o K for a factor of 2 increase in the heat-transfer coefficient.) Obviously, the higher the R/δ ratio and the lower the heat flux, the less will be the variation in resistivity in the power producing region.

It can be concluded that neglecting the temperature variation in properties should not have an appreciable effect on the analysis of a tungsten cylinder for the range of variables covered in this section. However, each material and each set of conditions must be checked to ensure that the property variation in the region of interest is small.

Negligible Internal Heat Generation

Another factor which could influence the accuracy of a heat-transfer test, using the method outlined in the section Application to Heat Transfer Testing, is the assumption that the heat generation in the region $r/R < 0.6$ is negligible. The validity of this assumption has qualitatively been established for large values of R/δ. A quantitative expression can also be obtained.

The heat conduction equation for the case of no internal heat generation in a thick-walled cylinder is given by equation (16) which can be rearranged and expressed in terms of the dimensionless temperature ratio (eq. (13)) as

$$\Delta T_c = \ln \frac{r}{a} \tag{19}$$

Comparison of equations (14) and (19) shows that the dimensionless temperature difference of the inductively heated cylinder (eq. (14)) is equal to that of the value of conduction case (eq. (19)) plus a correction term. Defining this correction term as α yields

$$\alpha = (\Delta T_i - \Delta T_c)$$

$$= \frac{1}{\epsilon}\left\{\frac{e^{X}\left[1 + X \ln\left(\frac{r}{a}\right)\right] - e^{xr/a} + \sum_{n=1}^{\infty} \frac{\left[\left(X \frac{r}{a}\right)^n - X^n\right]}{n \cdot n!} - \ln\left(\frac{r}{a}\right) \sum_{n=1}^{\infty} \frac{X^n}{n!}}{e^{y}(y - 1) + 1}\right\} \tag{20}$$

The ratio of the induction to conduction temperature distributions, which is a measure of

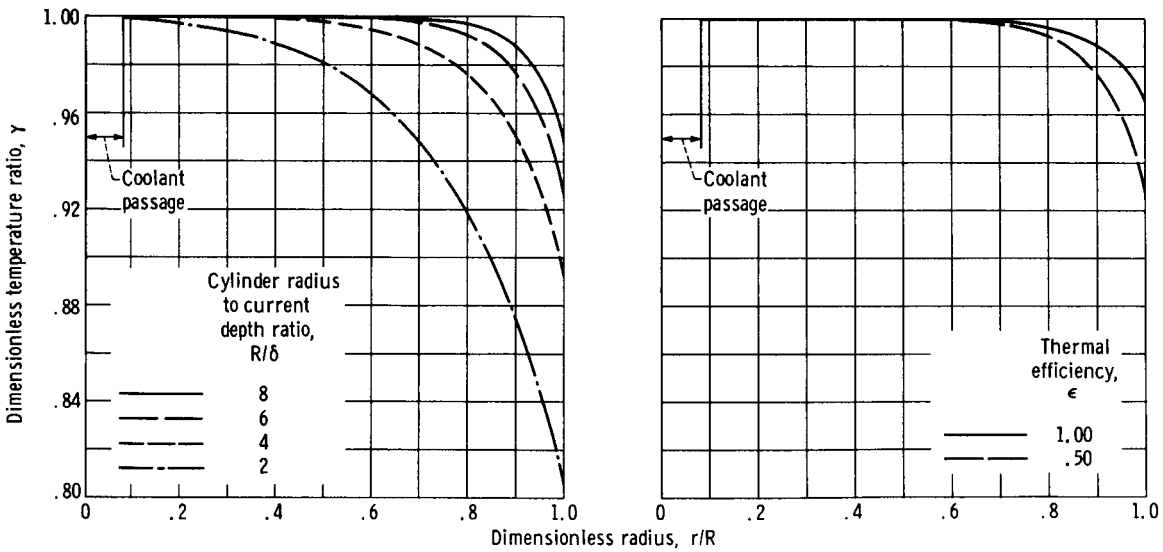

(a) Test section thermal efficiency, 0.50.

(b) Ratio of cylinder radius to current depth, 6.

Figure 14. - Effect of current depth on difference in radial temperature distribution between inductively heated and conductively heated cylinders. Ratio of cylinder radius to coolant-hole size, 12.

the importance of the internal heat generation, can be then written as

$$\gamma = 1 + \frac{\alpha}{\ln \frac{r}{a}} \tag{21}$$

Figure 14 shows plots of the dimensionless temperature ratio γ for several values of R/δ and ϵ. For values of R/δ greater than 6, the difference between the temperature distribution for the inductively heated cylinder and the conduction case are negligible in the region $r/R < 0.6$, and the internal heat generation can therefore be neglected in this region.

Experimental Errors

In addition to the aforementioned possible sources of error which could result from assumptions made in the analysis, there are also errors which could result from experimental inaccuracies. These errors include those resulting from measuring temperatures and temperature differences and those resulting from insufficient knowledge of thermocouple locations. Experimental errors are common to all heat-transfer tests of this nature and are not peculiar to the induction heating method. However, the fact that the thermocouples must be inserted axially (fig. 5) in the inductively heated test section could result in a somewhat larger error than if they were inserted radially.

The magnitude of the experimental errors can be determined by combining equations (15) to (17) into a dimensionless heat transfer coefficient

$$\frac{ha}{K} = \frac{1}{\left(\frac{T_2 - T_b}{T_2 - T_1}\right)\ln\left(\frac{r_2}{r_1}\right) - \ln\left(\frac{r_2}{a}\right)} \tag{22}$$

In addition to the desired heat-transfer coefficient, the left side of this equation contains the thermal conductivity of the test section and the radius of the coolant hole. Although these two parameters directly influence the accuracy of the experiment, they are essentially a part of the test section rather than the experimental measurements. The error resulting from these parameters will largely depend on how well the properties of the test section are known.

Grouped on the right side of the dimensionless relation (eq. (22)) are those factors which directly affect the experimental data. These include the location of thermocouples and the ability to measure temperatures and temperature differences. Figure 15(a)

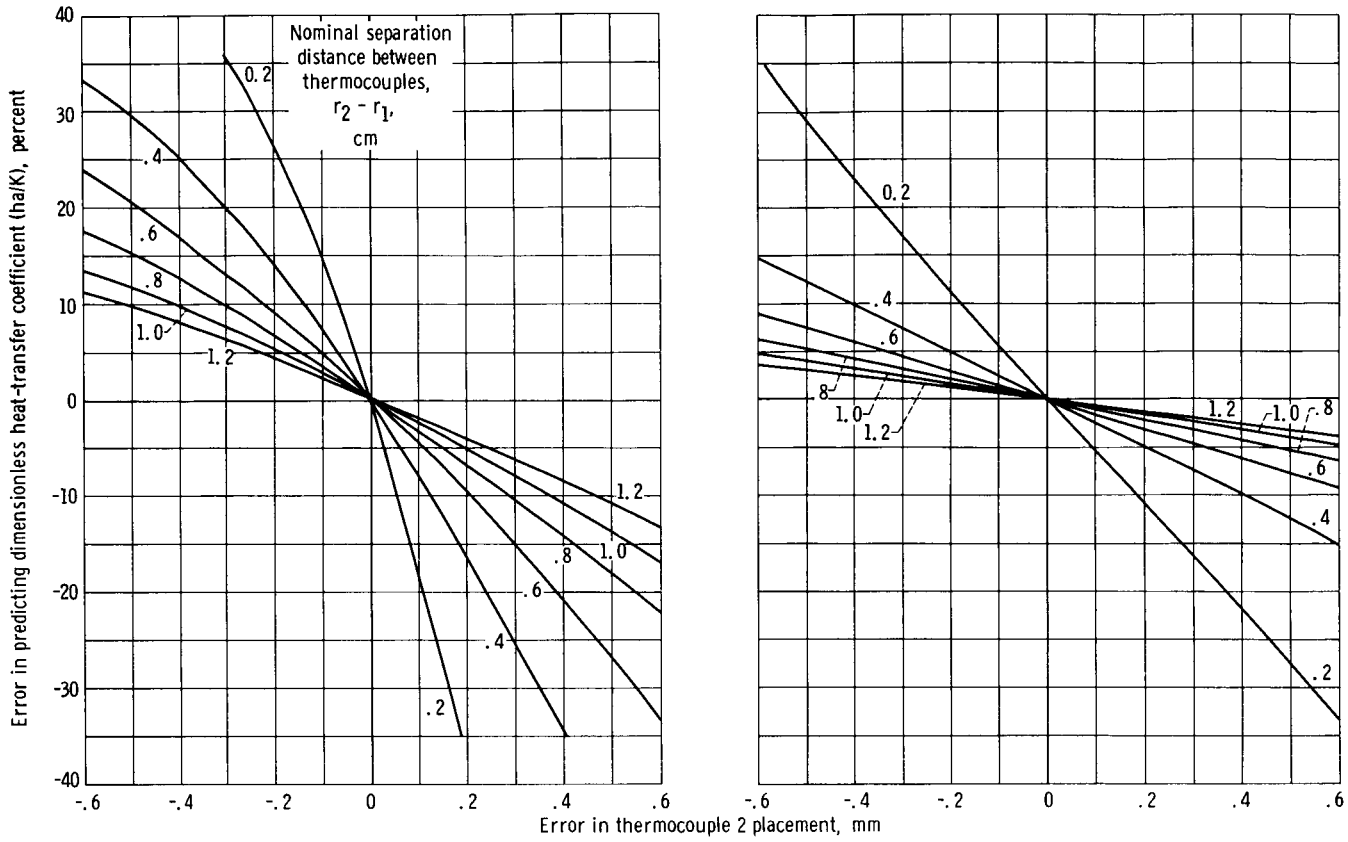

(a) Location of thermocouple 1, 1.15 centimeters.

(b) Location of thermocouple 1, 0.4 centimeter.

Figure 15. - Effect of error in thermocouple location on ability to predict heat-transfer coefficient from measured temperature difference. Radius of coolant channel, 0.32 centimeter; ratio of cylinder radius to current depth, 6; bulk fluid temperature, 1670° K; heat flux, 475 watts per square centimeter; thermal conductivity, 1.03 watts per square centimeter per °K.

shows how an error in thermocouple placement causes an error in the predicted value of (ha/K). These calculations were performed for an initial thermocouple placement (1) of r_1 = 1.15 centimeters and for various separation distances ($r_2 - r_1$). The more distance between the thermocouple locations, the less sensitive the data is to an error in thermocouple placement. Figure 15(b) shows that, by placing the thermocouples nearer the coolant hole (i.e., r_1 = 0.4 cm instead of 1.15 cm), the error is reduced considerably; for an error in thermocouple placement of -0.6 millimeter, for example, the error in predicting ha/K for a nominal separation distance of 1.0 centimeter is reduced from 13.5 to 5 percent for the conditions shown.

The effect of error in measuring temperature differences is shown on figure 16. Although the slopes are reversed, the magnitude of the error involved is essentially the same for either an error in ($T_2 - T_1$) or ($T_2 - T_b$). Since there are many possible combinations of errors in temperature measurements and thermocouple locations, it is impossible to estimate the exact error which would result in a typical experiment. Table V, however, shows the resulting error for several heat-flux levels and for all possible combinations of these errors assuming that the temperature differences could be measured to

TABLE V. - ERROR IN DETERMINING HEAT-TRANSFER COEFFICIENT OF INDUCTIVELY HEATED CYLINDER FOR VARIOUS COMBINATIONS OF ASSUMED EXPERIMENTAL TOLERANCES

Tolerance			Heat flux, W/cm^2		
Thermocouple location, Δr, mm	Temperature differential, ^{o}K		160	475	790
	$T_2 - T_1$	$T_2 - T_b$	Error in predicting dimensionless heat transfer coefficient (ha/K), percent		
0	0	0	-----	-----	-----
0	0	-3	+12.1	+3.7	+2.2
0	0	+3	-9.7	-3.5	-2.1
0	-3	0	-14.9	-5.4	-3.3
0	-3	-3	-5.8	-2.0	-1.2
0	-3	+3	-22.4	-8.5	-5.3
0	+3	0	+19.0	+5.8	+3.4
0	+3	-3	+35.7	+9.9	+5.8
0	+3	+3	+6.0	+2.0	+1.2
-.6	0	0	-3.8	-3.8	-3.8
-.6	0	-3	+7.8	-.2	-1.7
-.6	0	+3	-13.1	-7.1	-5.8
-.6	-3	0	-18.1	-8.9	-6.9
-.6	-3	-3	-9.5	-5.7	-4.9
-.6	-3	+3	-25.3	-12	-8.8
-.6	+3	0	+14.5	+1.8	-.5
-.6	+3	-3	+30.4	+5.7	+1.8
-.6	+3	+3	+2.1	-1.8	-2.6
+.6	0	0	+3.7	+3.7	+3.7
+.6	0	-3	+16.4	+7.6	+6.0
+.6	0	+3	-6.5	+.1	+1.5
+.6	-3	0	-11.7	-1.8	+.3
+.6	-3	-3	-2.2	+1.7	+2.5
+.6	-3	+3	-19.5	-5.2	-1.8
+.6	+3	0	+23.4	+9.7	+7.2
+.6	+3	-3	+41.0	+14.0	+9.7
+.6	+3	+3	+9.8	+5.7	+4.9
Range			+41 -25	+14 -12	+10 -9

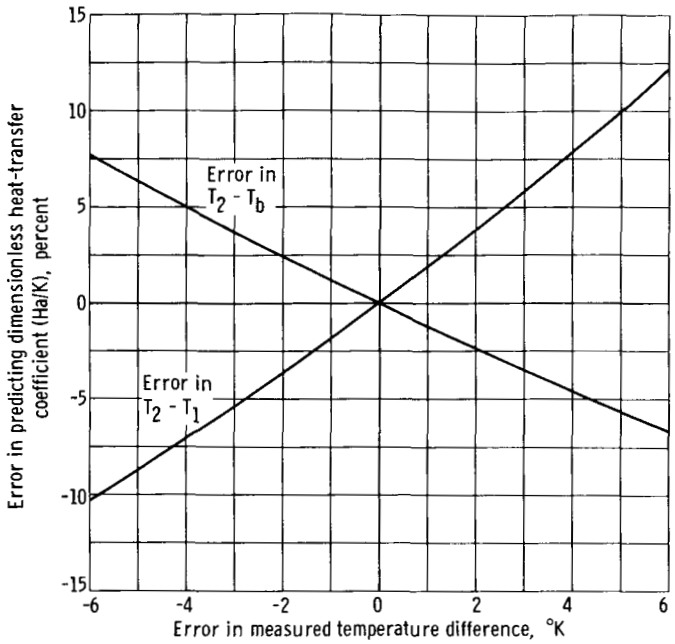

Figure 16. - Effect of error in measuring temperature on the ability to predict heat-transfer coefficient. Radius of coolant channel, 0.32 centimeter; location of thermocouple 1, 0.4 centimeter; distance between thermocouples 1 and 2; 1.2 centimeters; bulk fluid temperature, 1670° K; heat flux, 475 watts per square centimeter; thermal conductivity, 1.03 watts per square centimeter per °K.

$\pm 3^{\circ}$ K and that the location of the thermocouple $r_2 - r_1 = 1.2$ centimeters could be determined to ±0.6 millimeter. The range of errors for a heat flux of 790 watts per square centimeter is about ±10 percent, while that for 475 watts per square centimeter is 2 to 4 percent higher.

Based on these values, it would appear that an overall error of ±20 percent could be achieved if the thermal conductivity of the test section were reasonably established (e.g., to ±10 percent).

COMPARISON WITH THICK-WALLED RESISTANCE HEATING

Basically, the experimental errors involved in the thick-walled resistively heated test section are the same as those for the inductively heated case (figs. 15 to 17). However, an additional complication arises because of the temperature variation of the electrical resistivity. In the inductively heated case, the temperature variation in the region of maximum heat generation was small enough that the resistivity variation was negligible (fig. 13(c)). However, in the resistively heated test section, the heat is generated throughout the cylinder and the entire variation in the resistivity must be considered.

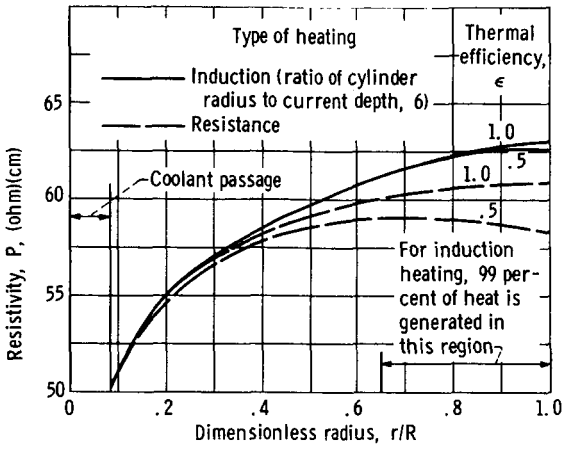

Figure 17. - Comparison of resistivity variation in tungsten cylinder heated by induction or resistance heating and cooled by liquid metal. Radius of coolant channel, 0.32 centimeter; ratio of cylinder radius to coolant-hole size, 12; heat flux, 475 watts per square centimeter; bulk fluid temperature, 1670° K; heat transfer coefficient, 6 watts per square centimeter per °K.

Figure 17 illustrates this point; the resistivity variation for an inductively and a resistively heated thick-walled cylinder are compared for a set of assumed operating conditions.

For the resistance heater, the variation in the electrical resistivity across the cylinder is between 18 and 23 percent depending on the thermal efficiency of the test section. In the inductively heated case, the variation in resistivity is less than three percent for the region in which 99 percent of the heat is generated. It is obvious that the result of neglecting resistivity variation will be much more significant for the resistively heated test section.

CONCLUDING REMARKS

Based on the analysis of an inductively heated, thick-walled cylinder, induction heating appears to offer a potential method of obtaining high temperatures (1000^{o} to 2000^{o} K) and high heat fluxes (400 to 1000 W/cm^2) for liquid-metal heat-transfer experiments. The analysis shows that, if the ratio of cylinder radius to equivalent current depth is greater than 6 and if the thermocouples are located in the region ($a/R < r/R < 0.6$), internal heat generation may be neglected. The resulting temperature distribution in this region is essentially the same as if the heat transfer through the cylinder were by conduction only.

Although no attempt was made to actually design a heating coil for the test section discussed in this report, it was assumed that a practical coil could be constructed which

would operate with a reasonable efficiency (e.g., 50 percent). Under these conditions, commercially available high-frequency equipment will adequately supply the power requirements for high heat-flux testing and provide the frequency necessary to achieve the desired cylinder radius to current depth ratios using a tungsten cylinder approximately 6 to 8 centimeters in diameter.

Assuming that the variation in electrical resistivity in a tungsten test section may be neglected does not affect the results of the analysis because the variation in temperature and resistivity is small in the region where the heat generation occurs. However, this assumption must be checked for a given set of conditions if materials other than tungsten are used or if the heat flux is very high.

Errors in the determination of the heat-transfer coefficient which are introduced by inaccurate thermocouple placement and temperature measurements are on the order of 10 to 15 percent over the heat flux range of interest (400 to 1000 W/cm^2). An additional error can also be introduced if the thermal conductivity of the test section is not well established.

Lewis Research Center,
National Aeronautics and Space Administration,
Cleveland, Ohio, October 2, 1967,
120-27-06-17-22.

APPENDIX A

SYMBOLS

a	radius of coolant channel, cm
ber, bei	defined parameters of J_0
C_1, C_2	constants of integration (appendix B)
C_p	specific heat at constant pressure, W-sec/(g)(^oK)
D	mathematical operator, d/dz
De	equivalent hydraulic diameter, cm
d	diameter of coolant channel, cm
F	geometric view factor for radiant heat transfer
f	frequency, Hz
G	mass flow rate, gm/(sec)(cm^2)
H	magnetic field intensity, A/cm
h	heat transfer coefficient, $W/(cm^2)(^oK)$
I	electrical current, A
J_0	Bessel function, first kind-order zero
j	imaginary unit, $\sqrt{-1}$
K	thermal conductivity, $W/(cm)(^oK)$
k	variable defined by eq. (3)
L	length of test section, cm
Nu	Nusselt number, hDe/K
n	integer 1, 2, 3, 4, . . .
P	electrical power, W
Pe	Péclet number, $GDeC_p/K$
Q	volumetric heat-generation rate, W/cm^3
q_ℓ	heat loss from outer surface of cylinder, W
q	heat generated, W
R	outer radius of cylinder, cm
R*	dimensionless distance, r/a
$\mathfrak{R}$	electrical resistance, ohms
r	arbitrary radius, cm
Δr	tolerance on thermocouple location, mm
T	temperature, ^oK
ΔT	dimensionless temperature difference, $K\left[T_{(r)} - T_a\right]/a\varphi_a$
ΔT^*	dimensionless maximum temperature difference, $K(T_{max} - T_a)/a\varphi_a$
x	dimensionless parameter, $2(a/\delta)$
y	dimensionless parameter, $2(R/\delta)$
α	dimensionless temperature difference, $\Delta T_i - \Delta T_c$
γ	dimensionless temperature ratio, $\Delta T_i/\Delta T_c$
δ	equivalent current depth, cm
ϵ	thermal efficiency of test section

μ	permeability, Wb/A-cm
ρ	resistivity, (ohm)(cm)
σ	Stefan-Boltzmann constant, 5.7×10^{-12} W/(cm^2)(^{o}K^4)
φ	heat flux, W/cm^2

Subscripts:

a	value at coolant surface
b	bulk fluid condition
c	conduction only
h	heater
i	induction heating
max	maximum value
n	nonferrous materials
o	outer surface of test section
o-r	region from center of cylinder to r
r	radius (variable)
r-R	region between r and R
T	temperature
t	total value
1, 2	thermocouple locations 1 and 2

APPENDIX B

DERIVATION OF EQUATIONS FOR INDUCTION HEATING OF CYLINDRICAL TEST SECTION FOR HIGH-TEMPERATURE HEAT-TRANSFER TESTING OF LIQUID METALS

Equation for Temperature Distribution in Cylindrical Body in Inductive Electrical Field

If it is assumed that the electrical resistivity of the material is constant, the approximate solution for the induced current distribution in a cylindrical body (ref. 19) is given by

$$\frac{I_{(r)}}{I_o} = e^{-(R-r)/\delta} \tag{B1}$$

for large values of R/δ, where $I_{(r)}$ is the current at any radial location and I_o the value at the surface of the cylinder. (The result of neglecting the resistivity variation is discussed in the main text.)

The power dissipated by the flow of current in a resistive element is

$$P = I^2\mathcal{R} \tag{B2}$$

where the electrical resistance $\mathcal{R}$ is proportional to the resistivity of the material and the length of the resistor and inversely proportional to the cross-sectional area of the resistor

$$\mathcal{R} = \rho(\text{length/area}) \tag{B3}$$

For the cylindrical shell (fig. 5), the geometry of the resistive element is

$$\text{area} = dr\ L$$

$$\text{length} \cong 2\pi r$$

$$\text{volume} \cong 2\pi r L\ dr$$

so that

$$\Re = \frac{2\pi r\rho}{L\ dr} \tag{B4}$$

and

$$P_{(r)} = \frac{2\pi r\rho}{L\ dr} I^2_{(r)} \tag{B5}$$

The volumetric heat-generation rate of the cylindrical shell is given by

$$Q_{(r)} = \frac{P_{(r)}}{\text{volume}} = \frac{P_{(r)}}{2\pi r L\ dr} \tag{B6}$$

Combining equations (B5) and (B6)

$$\left.\begin{aligned} Q_{(r)} &= \frac{2\pi r\rho I^2_{(r)}}{L\ dr\ 2\pi r L\ dr} \\ Q_{(r)} &= \frac{\rho}{(L\ dr)^2} I^2_{(r)} \end{aligned}\right\} \tag{B7}$$

Again neglecting temperature variations in the resistivity of the material, the volumetric heat-generation rate may be related to the induced current

$$\frac{Q_{(r)}}{Q_o} = \left[\frac{I_{(r)}}{I_o}\right]^2 \tag{B8}$$

or

$$Q_{(r)} = Q_o e^{-2(R-r)/\delta} \tag{B9}$$

Neglecting axial conduction and temperature variations in thermal conductivity, the basic heat conduction equation for a cylindrical body with internal heat generation is given by reference 24.

$$\frac{d^2T}{dr^2} + \frac{1}{r}\frac{dT}{dr} = -\frac{Q_{(r)}}{K} \tag{B10}$$

which, for the case of induction heating, becomes

$$\frac{d^2T}{dr^2} + \frac{1}{r}\frac{dT}{dr} = \frac{-Q_o e^{-2(R-r)/\delta}}{K} \tag{B11}$$

letting

$$A = \frac{-Q_o}{K} e^{-2R/\delta}$$

and

$$m = \frac{2}{\delta}$$

equation (B11) may be expressed as

$$\frac{d^2T}{dr^2} + \frac{1}{r}\frac{dT}{dr} = Ae^{mr} \tag{B12a}$$

or

$$r^2\frac{d^2T}{dr^2} + r\frac{dT}{dr} = Ar^2e^{mr} \tag{B12b}$$

This has the general form of the Cauchy linear differential equation which can be solved by letting

$$r = e^z$$

or

$$z = \ln r$$

Equation (B12) may then be rewritten as (ref. 27)

$$D(D - 1)T + DT = Ae^{2z}e^{me^z} \tag{B13}$$

where D is the mathematical operator d/dz. Expanding equation (B13) yields

$$(D^2 - D + D)T = Ae^{2z}e^{me^z}$$

$$D^2T = Ae^{2z}e^{me^z}$$

or

$$\frac{d^2T}{dz^2} = Ae^{2z}e^{me^z} \tag{B14}$$

The complementary solution of this equation is

$$T = C_1z + C_2 \tag{B15}$$

To obtain a particular solution, let

$$u = \frac{dT}{dz}$$

so that

$$\frac{du}{dz} = Ae^{2z}e^{me^z}$$

and

$$u = A\int e^{2z}e^{me^z}\,dz \tag{B16}$$

Letting

$$s = e^z$$

and

$$ds = e^z\,dz$$

equation (B16) can be written as

$$u = A\int se^{ms}\,ds$$

for which

$$u = A\left[\frac{e^{ms}}{m^2}(ms - 1)\right]$$

Therefore,

$$\frac{dT}{dz} = \left(\frac{A}{m^2}\right)\left[e^{me^z}(me^z - 1)\right]$$

and

$$T = \left(\frac{A}{m^2}\right)\int e^{me^z}(me^z - 1)dz \qquad \text{(B17)}$$

Again letting

$$s = e^z$$

$$ds = e^z\, dz$$

equation (B17) becomes

$$T = \left(\frac{A}{m^2}\right)\int\left(me^{ms} - \frac{e^{ms}}{s}\right)ds$$

so that

$$T = \left(\frac{A}{m^2}\right)\left\{e^{ms} - \left[\ln s + \sum_{n=1}^{\infty}\frac{(ms)^n}{n \cdot n!}\right]\right\}$$

By substituting for s, the particular solution is found to be

$$T = \left(\frac{A}{m}\right)^2\left\{e^{me^z} - \left[z + \sum_{n=1}^{\infty}\frac{(me^z)^n}{n \cdot n!}\right]\right\} \qquad \text{(B18)}$$

Combining the complimentary (eq. (B15)) and particular solution (eq. (B18)), the complete solution is given by

$$T_{(z)} = C_1 Z + C_2 + \left(\frac{A}{m^2}\right)\left[e^{me^z} - Z - \sum_{n=1}^{\infty} \frac{\left(me^z\right)^n}{n \cdot n!}\right] \tag{B19}$$

replacing Z by ln r, equation (B19) becomes

$$T_{(r)} = C_1 \ln r + C_2 + \left(\frac{A}{m^2}\right)\left[e^{mr} - \ln r - \sum_{n=1}^{\infty} \frac{(mr)^n}{n \cdot n!}\right] \tag{B20}$$

The previously substituted values of

$$A = -\frac{Q_o}{K} e^{-2R/\delta}$$

and

$$m = \frac{2}{\delta}$$

may be resubstituted at this time so that

$$T_{(r)} = C_1 \ln r + C_2 + \frac{Q_o}{K} e^{-2R/\delta} \left(\frac{\delta}{2}\right)^2 \left[\ln r - e^{2r/\delta} + \sum_{n=1}^{\infty} \frac{\left(2\frac{r}{\delta}\right)^n}{n \cdot n!}\right] \tag{B21}$$

The first derivative of this expression is also useful in the solution of the problem

$$\frac{dT}{dr} = \frac{C_1}{r} + \frac{Q_o}{k} e^{-2R/\delta}\left(\frac{\delta}{2}\right)\left[\frac{\delta}{2r} - e^{2r/\delta} + \sum_{n=1}^{\infty} \frac{\left(\frac{2r}{\delta}\right)^{n-1}}{n!}\right] \tag{B22}$$

The boundary conditions of interest in the problem of a liquid metal heat-transfer test are

$$\varphi_a = K\frac{dT}{dr} \qquad \text{at } r = a$$

and

$$T_a = T_{(r)} \qquad \text{at } r = a$$

When these boundary conditions are substituted into equations (B21) and (B22), the temperature distribution in the test section is

$$T_{(r)} - T_a = C_1 \ln\left(\frac{r}{a}\right) + \frac{Q_o}{K}\left(\frac{\delta}{2}\right)^2 e^{-2R/\delta}\left\{\ln\left(\frac{r}{a}\right) + e^{2a/\delta} - e^{2r/\delta} + \sum_{n=1}^{\infty}\left[\frac{\left(\frac{2r}{\delta}\right)^n - \left(\frac{2a}{\delta}\right)^n}{n \cdot n!}\right]\right\} \tag{B23}$$

where

$$C_1 = \varphi_a\left(\frac{a}{K}\right) + \frac{Q_o}{K}\left(\frac{\delta}{2}\right)^2 e^{-2R/\delta}\left[\left(\frac{2a}{\delta}\right)e^{2a/\delta} - 1 - \sum_{n=1}^{\infty}\frac{\left(2\,\frac{a}{\delta}\right)^n}{n!}\right]$$

Determination of Heat Generation Rate at Cylinder Surface

In the derivation of the temperature distribution in the cylinder, it was assumed that the value of Q_o, the heat generation rate at the outer surface of the cylinder, was known. However, the value of Q_o is dependent on several factors and must be related to these variables to obtain a complete solution to the problem.

The total heat generated in the cylinder by induction heating can be found by integrating the volumetric heating rate

$$q_t = \int_0^R 2\pi r L Q_{(r)}\, dr \tag{B24}$$

which on substituting the value of $Q_{(r)}$ and integrating becomes

$$q_t = 2\pi L Q_o \left(\frac{\delta}{2}\right)^2 \left(e^{-2R/\delta} + 2\frac{R}{\delta} - 1\right) \tag{B25}$$

In the same manner, the integrated heat input between any two arbitrary radial locations may be determined. The results for the regions of interest are

$$q_{o-r} = 2\pi L Q_o \left(\frac{\delta}{2}\right)^2 e^{-2R/\delta}\left[e^{2r/\delta}\left(2\frac{r}{\delta} - 1\right) + 1\right] \tag{B26}$$

so that

$$\frac{q_{o-r}}{q_t} = \left[\frac{e^{2r/\delta}\left(2\frac{r}{\delta} - 1\right) + 1}{e^{2R/\delta}\left(2\frac{R}{\delta} - 1\right) + 1}\right] \tag{B27}$$

and

$$\frac{q_{r-R}}{q_t} = 1.0 - \frac{q_{o-r}}{q_t} \tag{B28}$$

Since some heat may be lost from the outer surface of the cylinder by radiation, conduction, and convection, the total heat generated in the cylinder is the sum of the heat lost from the outer surface and that transferred to the liquid-metal coolant

$$q_t = 2\pi a L \varphi_a + q_l \tag{B29}$$

Defining the thermal efficiency of the test section as the ratio of heat received by the liquid-metal coolant to the total heat generated in the cylinder,

$$\epsilon = \frac{2\pi a L \varphi_a}{q_t} \tag{B30}$$

(This is different than the overall efficiency of the system where losses in other components must also be considered.) Using this relation, equation (B29) can be written as

$$q_t = \frac{2\pi a L \varphi_a}{\epsilon} \tag{B31a}$$

or

$$\frac{q_t}{2\pi L} = \frac{a\varphi_a}{\epsilon} \tag{B31b}$$

Substituting in equation (B25), the expression for Q_o is found in terms of the heat flux to the coolant

$$Q_o = \frac{a\varphi_a e^{2R/\delta}}{\epsilon\left(\frac{\delta}{2}\right)^2\left[e^{2R/\delta}\left(2\frac{R}{\delta} - 1\right) + 1\right]} \tag{B32}$$

Dimensionless Temperature Distribution

When equation (B32) is substituted into equation (B23), the complete solution for the temperature distribution is obtained

$$T_{(r)} - T_a = C_1 \ln\left(\frac{r}{a}\right) + \frac{a\varphi_a}{K\epsilon}\left[\frac{\ln\left(\frac{r}{a}\right) + e^{2a/\delta} - e^{2r/\delta} + \sum_{n=1}^{\infty} \frac{\left(\frac{2r}{\delta}\right)^n - \left(2\frac{a}{\delta}\right)^n}{n \cdot n!}}{e^{2R/\delta}\left(2\frac{R}{\delta} - 1\right) + 1}\right] \tag{B33}$$

where

$$C_1 = \frac{a\varphi_a}{K} + \frac{a\varphi_a}{K\epsilon}\left[\frac{\left(2\frac{a}{\delta}\right)e^{2a/\delta} - 1 - \sum_{n=1}^{\infty}\frac{\left(2\frac{a}{\delta}\right)^n}{n!}}{e^{2R/\delta}\left(2\frac{R}{\delta} - 1\right) + 1}\right]$$

Defining the dimensionless temperature difference

$$\Delta T = \frac{K\left[T_{(r)} - T_a\right]}{a\varphi_a} \tag{B34}$$

and rearranging equation (B33) yields an expression for the temperature distribution which is independent of the heat flux to the coolant and the thermal conductivity of the material.

$$\Delta T = \ln\left(\frac{r}{a}\right) + \frac{1}{\epsilon}\left\{\frac{e^x\left[1 + \ln\left(\frac{r}{a}\right)\right] - e^{xr/a} + \sum_{n=1}^{\infty}\frac{\left[\left(\frac{xr}{a}\right)^n - X^n\right]}{n\cdot n!} - \ln\left(\frac{r}{a}\right)\sum_{n=1}^{\infty}\frac{X^n}{n!}}{e^y(y-1)+1}\right\} \tag{B35}$$

where the dimensionless parameters x and y are given by

$$x = 2\frac{a}{\delta}$$

and

$$y = 2\frac{R}{\delta}$$

Determination of Maximum Temperature in Cylinder

The maximum temperature T_{max} in the cylinder will occur when

$$\frac{d(\Delta T)}{d\left(\frac{r}{a}\right)} = 0$$

By differentiating equation (B35), a transcendental expression for the location R^* of the maximum temperature difference ΔT^* is obtained

$$XR^*e^{XR^*} - \sum_{n=1}^{\infty} \frac{(XR^*)^n}{n!} = \epsilon\left[e^y(y - 1) + 1\right] + Xe^X - \sum_{n=1}^{\infty} \frac{X^n}{n!} \qquad \text{(B36)}$$

where $R^* = (r/a)$ at the location of maximum temperature. This equation may be solved graphically or by trial and error and the value of R^* substituted into equation (B33) to obtain the expression for the maximum temperature difference

$$\Delta T^* = \ln(R^*) + \frac{1}{\epsilon}\left\{\frac{e^X\left[1 + X\ln(R^*)\right] - e^{XR^*} + \sum_{n=1}^{\infty} \frac{\left[(XR^*)^n - X^n\right]}{n \cdot n!} - \ln(R^*) \sum_{n=1}^{\infty} \frac{X^n}{n!}}{e^y(y - 1) + 1}\right\} \qquad \text{(B37)}$$

REFERENCES

1. DeMastry, John A.: Liquid Metals in Space Power Systems. Battelle Tech. Rev., vol. 15, no. 3, Mar. 1966, pp. 17-21.

2. Green, Leon: Reactor-Coolant Properties. Nucleonics, vol. 19, no. 11, Nov. 1961, pp. 140-144.

3. Kummerer, K.: Selection of Liquid Metals in Reactor Technology. Atomkernenergie, vol. 9, no. 5-6, 1964, pp. 159-165.

4. Martinelli, R. C.: Heat Transfer to Molten Metal. Trans. ASME, vol. 69, no. 8, Nov. 1947, pp. 947-959.

5. Lyons, Richard N., ed.: Liquid-Metals Handbook. Second ed. Rep. No. NAVEXOS-P-733 (Rev.), Office of Naval Research and AEC, June 1952, pp. 185-187.

6. Seban, R. A.; and Shimazaki, T. T.: Heat Transfer to a Fluid Flowing Turbulently in a Smooth Pipe with Walls at Constant Temperature. Trans. ASME, vol. 73, no. 6, Aug. 1951, pp. 803-809.

7. Lubarsky, Bernard; and Kaufman, Samuel J.: Review of Experimental Investigations of Liquid-Metal Heat Transfer. NACA TN-3336, 1955.

8. Kutateladze, S. S.; Borishansky, V. M.; and Novikov, I. I.: Heat Transfer in Liquid Metals. Atomnaya Energiya, vol. 4, 1958, pp. 422-436.

9. Lottes, Paul A.: Nuclear Reactor Heat Transfer. Rep. No. ANL-6469, Argonne National Lab., Dec. 1961, p. 81.

10. Viskanta, R.; and Touloukian, Y. S.: Heat Transfer to Liquid Metals with Variable Properties. J. Heat Transfer, vol. 82, no. 4, Nov. 1960, pp. 333-340.

11. Taylor, Maynard F.: Experimental Local Heat-Transfer Data for Precooled Hydrogen and Helium at Surface Temperatures up to 5300° R. NASA TN D-2595, 1965.

12. DeBortoli, R. A ; Green, S. J.; LeTourneau, B. W.; Troy, M.; and Weiss, A.: Forced-Convection Heat Transfer Burnout Studies for Water in Rectangular Channels and Round Tubes at Pressures Above 500 PSIA. Rep. No. WAPD-188, Westinghouse Electric Corp., Oct. 1958.

13. Lottes, Paul A.: Applying High-Temperature Instrumentation in Liquid-Metal Experiments. Power Reactor Tech., vol. 9, no. 3, summer 1966, pp. 123-136.

14. Hayward, B. R.; Babbe, E. L.; and Darley, D. K.: High Heat Flux Heater Development Preliminary Performance Tests. Rep. No. NAA-SR-12242, Atomics International, Dec. 31, 1966.

15. Geidt, Warren H.: Principles of Engineering Heat Transfer. D. Van Nostrand Co., Inc., 1957, p. 255.

16. Kalachev, D. M.; Kudryavtsev, I. S.; Paskar', B. L.; and Yakubovich, I. I.: High-Frequency Induction Heating of Liquid-Metal Heat-Transfer Agents. Proceedings of the Second All-Soviet Union Conference on Heat and Mass Transfer. Vol. 1. C. Gazley, Jr., J. P. Hartnett, and E. R. G. Eckert, eds. Rep. No. R-451-Pr, vol. 1, Rand Corp. California University Press, 1966, pp. 61-64.

17. Anon.: High-Frequency Induction Heating Equipment. Bulletin E 110/7-65, Lepel High Frequency Laboratories, Inc.

18. Anon.: High Frequency Motor-Generators. Bulletin DB-2001-4-65, TOCCO Div., Ohio Crankshaft Co.

19. Simpson, P. G.: Induction Heating: Coil and System Design. McGraw-Hill Book Co., Inc., 1960.

20. Knowlton, Archer E., ed.: Standard Handbook for Electrical Engineers. Ninth ed., McGraw-Hill Book Co., Inc., 1957, sect. 18-116, p. 1793.

21. Weast, Robert C., ed.: Handbook of Chemistry and Physics. 37th ed., Chemical Rubber Publishing Co., 1955, pp. 2357-2360.

22. Abramowitz, Milton; and Stegun, Irene A., eds.: Handbook of Mathematical Functions with Formulas, Graphs, and Mathematical Tables. Appl. Math. Ser. No. 55, National Bureau of Standards, June 1964, pp. 430-432.

23. Jahnke, Eugene; and Emde, Fritz: Table of Functions with Formulae and Curves. Fourth ed., Dover Publications, 1945.

24. Eckert, E. R. G.; and Drake, Robert M., Jr.: Heat and Mass Transfer. Second ed., McGraw-Hill Book Co., Inc., 1959.

25. Fiero, Ivan B.: Establishing Allowable Temperature Gradients for Tungsten - Uranium Dioxide Fuel Elements Using Experimental Cyclic Strain Data. NASA Technical Note; estimated publication date, December 1967.

26. Miller, John V.: Estimating Thermal Conductivity of Cermet Fuel Materials for Nuclear Reactor Application. NASA TN D-3898, 1967.

27. Ayres, Frank: Schaum's Outline of Theory and Problems of Differential Equations. Schaum Publishing Co., 1952, p. 108.

NASA-Langley, 1968 — 33 E-3894